

WESTERN DELTA SALINITY MODELING USING ARTIFICIAL NEURAL NETWORKS

Draft Final Report

Prepared for:

**Paul Hutton, Ph.D., P.E.
Metropolitan Water District of Southern California
1121 L Street, Suite 900
Sacramento CA 95814-3974**

Prepared by:

**Limin Chen and Sujoy B. Roy
Tetra Tech Inc.
3746 Mt. Diablo Blvd, Suite 300
Lafayette, CA 94549**

April 11, 2013

TABLE OF CONTENTS

1. Introduction	1-1
2. Approach	2-1
2.1 Data Types Used	2-1
2.2 Artificial Neural Network (ANN) Models	2-1
2.2.1 Model Inputs.....	2-1
2.2.2 ANN Output Locations.....	2-2
2.2.3 ANN Model Structure.....	2-3
2.2.4 Training Approach	2-5
2.3 Model Input Data.....	2-5
2.3.1 Flow.....	2-5
2.3.2 Tide	2-6
2.3.3 Salinity.....	2-6
2.3.4 Channel Depth	2-7
2.4 Description of G-Model	2-13
2.5 Description of K-M Model.....	2-13
2.6 DSM-2 Model	2-13
3. Results	3-1
3.1 ANN Network Training Results.....	3-1
3.1.1 Flow Variables.....	3-1
3.1.2 Tide Variables	3-2
3.1.3 Antecedent Salinity Input.....	3-3
3.1.4 Overall Model Performance.....	3-4
3.1.5 Time Delay	3-6
3.1.6 Channel Depth	3-7
3.2 Comparison of Results to G-model	3-9
3.3 ANN Models for Specific Stations	3-11
3.4 Use of Trained Network in X2 Calculations.....	3-12
3.5 Comparison to K-M model	3-14
3.6 Comparison with DSM2 Model.....	3-17
3.7 Sensitivity Analysis and Changes due to Sea Level Rise	3-20
3.8 Sensitivity to Air Pressure and Qwest Flow.....	3-23
3.9 Changes in X2 due to Sea Level Rise.....	3-24
3.10 Application to Historical Salinity Data.....	3-24
3.11 Distance-Salinity Projections using a Trained ANN Model.....	3-31
3.12 Long Term Salinity Projections using Feedforward and Autoregressive Models	3-32
4. Summary and Recommendations	4-1

5. References..... 5-1
Appendix A Correlations Used to Fill Data Gaps in CDEC Stations
Appendix B Processes Used to Fill Data Gaps in Bay Stations
Appendix C Correlations of Astronomical Tide and Meteorological Variables
Appendix D Training Results
Appendix E Comparison of Training with and without Channel Depth

LIST OF FIGURES

Figure 2-1	Locations of output stations for ANN training. Three letter codes, where shown, refer to CDEC and USGS station codes.	2-3
Figure 2-2	Daily Rio Vista flow from IEP DAYFLOW.	2-8
Figure 2-3	Daily Qwest flow from IEP DAYFLOW.	2-8
Figure 2-4	Correlation between Rio Vista flow and Qwest flow.	2-9
Figure 2-5	Tidal Range at Golden Gate.	2-9
Figure 2-6	Correlation between residuals (difference between actual tide and astronomical tide) and air pressure at Golden Gate (Data source: NOAA).	2-10
Figure 2-7	Cleaned and filled EC data at Collinsville (CLL).	2-10
Figure 2-8	Cleaned and filled EC data at Emmaton (EMM).	2-11
Figure 2-9	Cleaned and filled EC data at Mallard Island (MAL).	2-11
Figure 2-10	Cleaned and filled EC data at Carquinez (CAR) and Point San Pablo (PSP).	2-12
Figure 2-11	Channel Depth in Suisun Bay (Source: CDFG).	2-12
Figure 3-1	G-model performance at Collinsville (CLL).	3-9
Figure 3-2	G-model performance at Port Chicago (PCT).	3-10
Figure 3-3	G-model performance at Jersey Point (JER).	3-10
Figure 3-4	Comparison of X2 calculated from the ANN model and the observed X2 for the Sacramento River stations.	3-13
Figure 3-5	Comparison of X2 calculated from the ANN model to the observed X2 for the San Joaquin River stations.	3-14
Figure 3-6	Comparison of X2 position calculated from K-M equation and the observed X2 for the Sacramento River stations.	3-15
Figure 3-7	Comparison of X2 calculated from the K-M equation and the observed X2 for the San Joaquin River stations.	3-16
Figure 3-8	Comparison of X2 position calculated from K-M model to the ANN models for the Sacramento River and the San Joaquin River stations.	3-17
Figure 3-9	Comparison of observed daily salinity to values calculated by the DSM-2 and ANN models for the EMM and JER stations, shown as a time	

series (beginning October 1, 1974) and scatterplot. DSM-2 values were available for a 20-year period from 1990-2010.....	3-18
Figure 3-10 Comparison of X2 calculated from the DSM2 model to the observed X2 (Sacramento River).....	3-19
Figure 3-11 Comparison of X2 calculated from the DSM2 model to the observed X2 (San Joaquin River).....	3-20
Figure 3-12 Projected EC over distance under different Rio Vista flow conditions (1000, 5000, 10000, 25000, and 50000 cfs).....	3-21
Figure 3-13 Projected EC as a function of standardized distance (X/X2) under different flow conditions.....	3-22
Figure 3-14 Projected EC over distance due to sea level rise of 1 feet and 2 feet under different Rio Vista flow conditions (1000, 10000 and 50000 cfs). Black: base, blue: 1 ft rise, red: 2 ft rise.	3-22
Figure 3-15 Values of sea level used as an input for training. The green and purple lines refer to a change of 1 foot and 2 feet respectively.	3-22
Figure 3-16 Sensitivity of salinity to air pressure (1000, 1015, 1030 mbar), for three different values of Rio Vista flow (1,000, 10,000, and 50,000 cfs).	3-23
Figure 3-17 Sensitivity of salinity to Qwest flow (mean using relationship between Qwest and Rio Vista flow, mean-14000 cfs, mean + 14000 cfs).....	3-24
Figure 3-18 Changes in X2 position due to sea level rise of 20 inches.....	3-24
Figure 3-19 Comparison of ANN simulated and reconstructed historical salinity at ANH, MRZ, and PCT.....	3-26
Figure 3-20 Comparison of ANN simulated and reconstructed historical salinity at JER and SAL.....	3-27
Figure 3-21 Comparison of ANN simulated and reconstructed historical salinity at CLL, EMM and RVB.....	3-28
Figure 3-22 Comparison of ANN simulated and reconstructed historical salinity at ANH, MRZ and PCT.....	3-29
Figure 3-23 Comparison of ANN simulated and reconstructed historical salinity at JER and SAL.....	3-30
Figure 3-24 Comparison of ANN simulated and reconstructed historical salinity at CLL, EMM and RVB.....	3-31
Figure 3-25 Comparison of feedforward ANN (Model 3) forecast and observed salinity from 0 to 150 days.....	3-32
Figure 3-26 Comparison of feedforward ANN (Model 3), upper panel, and autoregressive ANN (Model 9), lower panel, forecast for a 10-year period starting October 1, 1974 (CLL station).	3-33

Figure 3-27 Comparison of feedforward ANN (Model3), upper panel, and autoregressive ANN (Model 9), lower panel, forecast for a 10-year period starting October 1, 1974 (EMM station). 3-34

Figure 3-28 Comparison of feedforward ANN (Model 3), upper panel, and autoregressive ANN (Model 9), lower panel, forecast for a 10-year period starting October 1, 1974 (MAL station). 3-35

Figure 3-29 Comparison of feedforward ANN (Model 3), upper panel, and autoregressive ANN (Model 9), lower panel, forecast for a 10-year period starting October 1, 1974 (MRZ station). 3-36

LIST OF TABLES

Table 2-1 Candidate ANN Model Structures Evaluated Following Initial Screening..... 2-5

Table 3-1 Comparison of Observations and ANN Model Outputs (*r*) for Evaluating
Flow Terms 3-2

Table 3-2 Comparison of Models Regarding Tide 3-3

Table 3-3 Comparison of Models on Antecedent salinity Input 3-4

Table 3-4 Performance of Trained Salinity ANN Model (Model 3) at Different
Locations..... 3-6

Table 3-5 Comparison of Training Results with Different Time Delays 3-7

Table 3-6 Comparison of Training Results With and Without Consideration of
Depth 3-8

Table 3-7 Comparison of Channel Depth Effects Added to Model 3 3-8

Table 3-8 Comparison of Model Performance to G-model 3-11

Table 3-9 Comparison of Selected Distance-Salinity ANN Models, Station-
Specific ANN models, and G-model..... 3-12

Table 3-10 Standard Error (km) Associated with X2 Estimation..... 3-20

ACRONYMS

ANN	Artificial Neural Network
DSM2	Delta Simulation Model II
CDEC	California Data Exchange Center
CDFG	California Department of Fish and Game
DWR	Department of Water Resources
FFW	Feed Forward Network
IEP	Interagency Ecological Program
MLP	Multi-layer Perceptron
MSL	Mean Sea Level
NARX	Nonlinear Autoregressive Network with Exogenous Inputs
SE	Standard Error
USGS	United States Geological Survey

1. INTRODUCTION

The abundance of several biological populations in the eastern reaches of San Francisco Estuary (Western Delta) is related to the location of the low salinity zone, which in turn depends on freshwater outflows from the Delta (Jassby et al. 1995). The position of the 2 parts per thousand (ppt) bottom salinity isohaline, termed X2, is a key component of the salinity standard in the estuary (US EPA, 1995). Under current regulations, it is interpolated as an equivalent surface salinity from fixed monitoring stations and reported as a distance from Golden Gate Bridge. Besides the X2 position, which is largely driven by habitat considerations, there are also salinity compliance points further east in the Delta for municipal and agricultural uses. Salinity behavior in an environment such as San Francisco Bay is known to be dynamic, and dependent on tides as well as current and antecedent freshwater flows (Harder, 1977; Denton and Sullivan, 1993). In support of inflow management in the Western Delta, there is a need to develop predictive tools that provide information on salinity at specific locations and the X2 position as a function of other inputs that can be predicted or defined.

In previous work, four types of predictive tools for X2 and/or salinity have been applied for different purposes:

- Autoregressive equation between Delta outflow and X2 position, termed the K-M model (Kimmerer and Monismith, 1992; Jassby et al., 1995);
- Salinity-antecedent flow relationship based on an approximate solution to the one-dimensional advection-dispersion equation for salt transport, termed the G-model (Denton and Sullivan, 1993);
- Numerical models of hydrodynamics and salinity, for example, one-dimensional linked-node modeling of hydrodynamics and salinity of the Delta using the California Department of Water Resources' (DWR) Delta Simulation Model (DSM-2), and three-dimensional modeling for salinity and flow in the entire bay and estuary (Gross et al., 2007, 2010);
- Artificial neural networks (ANNs) to represent flow and salinity in the Delta (Finch and Sandhu, 1995; Wilbur and Munevar, 2001; Mierzwa, 2002; Seneviratne et al., 2008).

The K-M model and the G-model are relatively straightforward expressions that have been used within planning models to evaluate compliance with salinity standards in the estuary. The DSM-2 model has been set up and calibrated to compute salinity across the entire Delta with the western boundary at Martinez. The DSM-2 model is used extensively for DWR's annual reporting to the State Water Resources Control Board. The more detailed three-dimensional solutions have been used to understand the depth-dependent behavior of salinity

under different flow and tidal conditions in San Francisco Bay and Delta region, although the computational demands of the models limits application within planning simulations that run over many years. The ANN approach has also been used extensively by DWR to represent salinity at different locations in the Delta, with the ANNs being trained on synthetic data being generated from DSM-2. Because ANNs run significantly faster than the mechanistic models they are trained on, they can be employed within planning models, where there is a need to return results rapidly. In contrast with prior applications, the present work is focused on the development of ANNs using observed data, as opposed to model output.

Although ANNs have a demonstrated record of describing complex hydrologic and water quality behavior (Maier et al., 2010; American Society of Civil Engineers, 2000), considerable testing and refinement is needed for a specific application, including identification of a suitable network structure, appropriate inputs, and time lags. Furthermore, ANNs are data-driven formulations, with the best performance occurring in the space over which the training has been performed, and with undefined performance when extrapolated beyond the training space. For this reason, it is beneficial to perform the training with the largest possible data set to assure that a wide variety of conditions are represented. In the present work, a set of ANN models for salinity for the western Delta and the estuary was developed using observed salinity data over nearly four decades, averaged to a daily time step. Multiple ANN formations were considered to evaluate performance over a range of inputs, and to allow selection of a model that balances input complexity and performance. The inputs considered included flows, tide terms, and channel depth. Two types of models were developed: one set that was focused on predicting salinity in the estuary based on distances from Golden Gate, and a second set focused on individual stations, not accounting for distance. The models can be applied to predict salinity at a specific location or as a function of distance; the latter information can be used to interpolate the values of X2.

The remaining sections of this report describe the data and approach used (Chapter 2); results from the different ANN models, comparison against existing tools and exploration of sensitivity of specific inputs such as flows and sea level (Chapter 3); and a summary of key findings and recommendations on the use of selected models in future applications (Chapter 4).

2. APPROACH

Multiple ANNs were trained using combinations of inputs (flow, tide, and channel depth) to evaluate which set of inputs adequately explain salinity behavior in the San Francisco estuary. The results of the training are individual ANNs that predict salinity as a function of distance for the Sacramento and San Joaquin Rivers, based on inputs of flow and tide. For efficient screening across a large number of models, the coefficient of correlation between the observed data at fixed locations and the model results (r) was used for comparison. ANN model results were compared with salinity estimation approaches used in previous work in the Delta, including the Kimmerer-Monismith equation (K-M equation, Kimmerer and Monismith, 1992), the G-model (Denton and Sullivan, 1993; Denton, 1993), and DSM-2 calculations for 1990-2010 (Sandhu, 2011, personal communication).

2.1 DATA TYPES USED

Salinity data, in the form of surface salinity reported as electrical conductance at 25 °C (EC in units of $\mu\text{S}/\text{cm}$) were used to train the model. The data were obtained from the California Data Exchange Center (CDEC), the Interagency Ecological Program (IEP), and US Environmental Protection Agency's STORET database (short for STOrage and RETrieval). Data were obtained for a set of fixed stations in the western Delta and San Francisco Bay. Additional data for stations in the Bay were also obtained from the US Geological Survey (USGS) (Carquinez and Point San Pablo). Other inputs used to train the ANN models included flow data obtained from DWR's DAYFLOW program, daily tide data obtained from the National Oceanic and Atmospheric Administration (NOAA), channel depth data obtained from the California Department of Fish and Game (CDFG), and distance from Golden Gate computed using station coordinates and measured along a line running down the mid-depth of the estuary. Specifics relating to the data used for training are described below.

2.2 ARTIFICIAL NEURAL NETWORK (ANN) MODELS

2.2.1 Model Inputs

The ANN models used in the training considered combinations of different input variables including:

- Station distance (km) from Golden Gate
- Channel depth – average annual values obtained from California Department of Fish and Game trawls
- Flow variables – Rio Vista flow (on the Sacramento River), Qwest flow (on the San Joaquin River past Jersey Point), and net Delta outflow from the DAYFLOW program
- Tides – Martinez and Antioch half tide, and Golden Gate tide, obtained from DWR and NOAA

Different time-delays for the flow and tide inputs were also explored, where a delay of n days refers to the use of 1 through n preceding days of inputs. Thus, a flow delay of 30 days refers to the use of flows from the previous 1 through 30 days (30 individual values) as input. In most of these model structures, salinity was calculated as a function of distance using the boundary inputs with a variable time delay. In a limited number of cases, we explored the role of antecedent salinity (as an additional input) in improving the quality of the fit. We also explored the development of station-specific ANNs, particularly for stations that were important from the compliance perspective and where the distance-based ANNs did not perform as well.

2.2.2 ANN Output Locations

For each input set, two separate ANN models were developed for the lower Sacramento River and lower San Joaquin River stations. The training was performed at fixed stations as a function of distance for either river, with the ANN output being available at any arbitrary distance within the range of distances considered. Training stations for the Sacramento River ANN model were salinity at a number of locations along the lower Sacramento River and several stations in the Bay. These include the following (station codes and distances from Golden Gate as computed by us along the center-depth of the estuary):

- Point San Pablo (PSP, 22 km)
- Carquinez (CAR, 45.5 km)
- Martinez (MRZ, 54.8 km)
- Port Chicago (PCT, 66.1km)
- Mallard Island (MAL, 76 km)
- Collinsville (CLL, 82.9 km)
- Emmaton (EMM, 93.0 km)
- Decker Island (SDI, 93.9 km)
- Rio Vista (RVB, 102.7 km)

Training stations for the San Joaquin River ANN model were salinity at a number of locations along the lower San Joaquin River and several stations in the Bay. These include the following, using the same format as for the Sacramento River stations:

- Point San Pablo (PSP, 22 km)
- Carquinez (CAR, 45.5 km)
- Martinez (MRZ, 54.8 km)
- Port Chicago (PCT, 66.1)
- Mallard Island (MAL, 76 km)
- Pittsburg (PTS, 80.2 km)
- Antioch (ANH, 87.3 km)

- Blind Point (BLP, 94.7 km)
- Jersey Point (JER, 98.7 km)
- Threemile Slough @ SJR (TSL, 103.3 km)
- San Andreas Landing (SAL, 112.9 km)

The locations of these stations are shown in Figure 2-1. Note that for the overlapping part of the two river models, ANN output can be generated from either model.

Besides the distance-salinity models, for selected stations, station-specific ANN models were also developed.

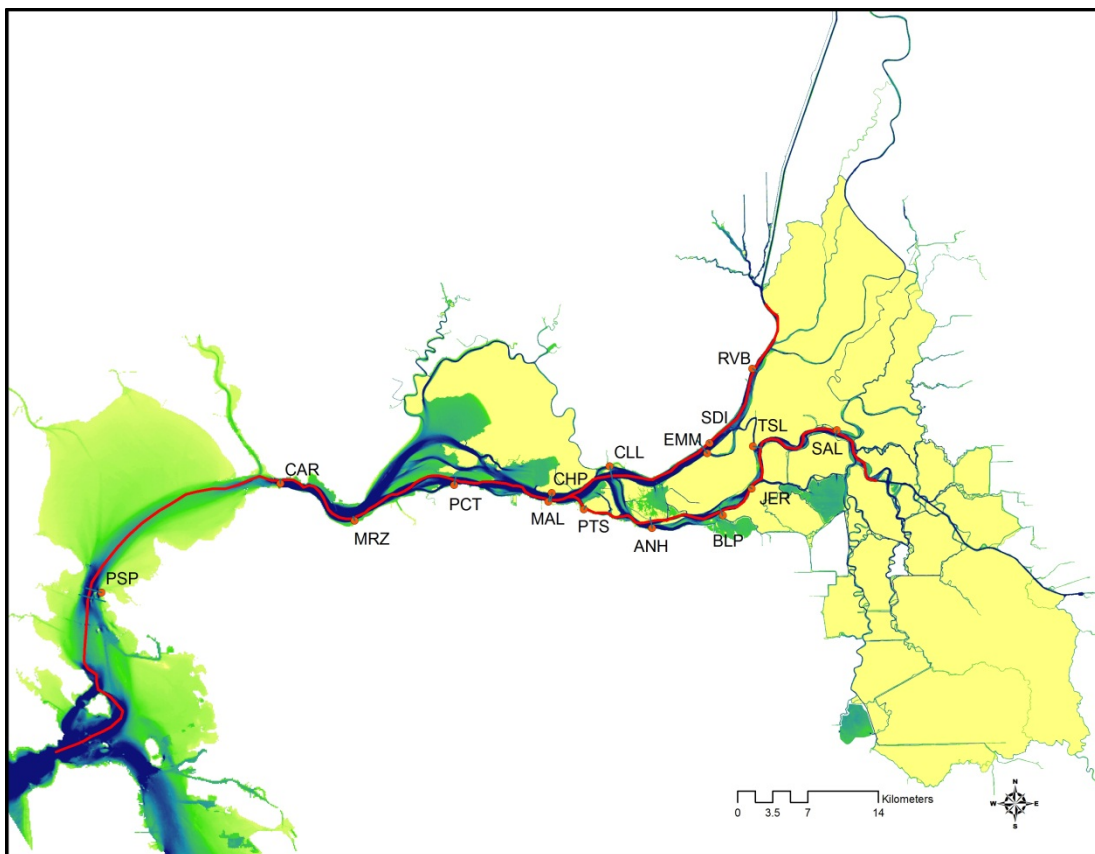


Figure 2-1 Locations of output stations for ANN training. Three letter codes, where shown, refer to CDEC and USGS station codes.

2.2.3 ANN Model Structure

The dynamic nature of flow and salinity in the Delta requires a network structure that takes into account the time-series of inputs. Although other network structures have received attention in the recent literature, the multi-layer perceptrons (MLPs) are by far the most popular network structures used in water resource applications to date, representing more than 90% of the peer-reviewed applications in the water resources field (Maier et al. 2010). For this reason, the feedforward MLP network was selected for this application.

For much of this analysis, ANNs were developed by accounting for station distance (integrating all stations along a river); based on the results of these salinity-distance ANNs, ANNs were developed focused on a set of specific stations.

Different network structures with respect to the number of input variables and lengths of time delay were explored, to evaluate factors that may affect salinity in the estuary. Assuming a range on inputs related to flow (3 inputs), tide (5 inputs), time lags (4 inputs), and channel depth (2 inputs, either considered or not), results in 120 possible combinations of models to be trained and evaluated for each river. In this work, a screening effort was used to identify a subset of candidate models for more detailed examination.

In the first step, models with different time delays were explored ranging from 7 days to 60 days. A 30-day time delay was shown to provide good results and was the basis of subsequent modeling. Time delays shorter than this showed slightly poorer fits, and increasing the time delay to 60 days showed little improvement for the distance-salinity ANN. Furthermore, there was a practical constraint in the computational time taken for performing training with longer delays. For these reasons, a 30-day delay was identified as a reasonable balance for representing the system memory and the training time constraint.

The depth effect was investigated separately, and was motivated by a recent evaluation from MWD (David Fullerton, personal communication) which suggested that changing bed depth may be relevant in explaining the discrepancies between salinity and flow relationships at certain locations (e.g., Collinsville). Although the depth term was not retained after the screening process, key results are summarized in Chapter 3 for future reference.

Flow terms included in the model were net Delta outflow, flow at Rio Vista (on the Sacramento River), and the Qwest flow (representing San Joaquin River flow at Jersey Point), all of which were obtained from the DAYFLOW model. The models were implemented using a single flow term (net Delta outflow), two flow terms (Rio Vista flow and Qwest flow), and using the Rio Vista flow plus a residual from the correlation between Rio Vista and Qwest flows. The last of these inputs provides additional information to the model, reflecting the correlation between the flows in the two major rivers.

The importance of tidal effects on salinity was evaluated by using different numbers of tidal terms in the training (from three tidal terms to no tidal terms) and using actual tide or the astronomical tide plus a residual term between the actual and astronomical tide. The consideration of these variables resulted in a total of 10 ANN models to be evaluated for the distance-salinity relationships (Table 2-1).

The model inputs evaluated in Table 2-1 also served as the basis for a limited assessment of the station-specific ANNs. The station-specific ANNs were limited to locations where the distance-based ANNs did not provide fits that were of high quality, and which are also important from the standpoint of water quality compliance.

**Table 2-1
Candidate ANN Model Structures Evaluated Following Initial Screening**

Number	Flow	Tides	Antecedent salinity Data as Input	Time Delay
1	Net Delta Outflow	Astronomical tide, residuals with actual tide	No	30
2	Rio Vista Flow, Qwest Flow	Astronomical tide, residuals with actual tide	No	30
3	Rio Vista Flow, Qwest as f (Q_{Rio})	Astronomical tide, residuals with actual tide	No	30
4	Rio Vista Flow, Qwest as f (Q_{Rio})	Three tidal terms (tidal range at Golden Gate and Martinez, and half tide at Mallard Island)	No	30
5	Rio Vista Flow, Qwest as f (Q_{Rio})	Two tidal terms (tidal range at Golden Gate and Martinez)	No	30
6	Rio Vista Flow, Qwest as f (Q_{Rio})	One tidal term (tidal range at Golden Gate)	No	30
7	Rio Vista Flow, Qwest as f (Q_{Rio})	No tidal term	No	30
8	Rio Vista Flow, Qwest as f (Q_{Rio})	Actual tide (MSL at Golden Gate)	No	30
9	Rio Vista Flow, Qwest as f (Q_{Rio})	Astronomical tide, residuals with actual tide	Yes	30
10	Rio Vista Flow, Qwest as f (Q_{Rio})	Astronomical tide, residuals with actual tide	NARX	30

2.2.4 Training Approach

In this work, the data were divided in the following manner: 60%, 20%, and 20% for training, validation and testing, respectively. The training and validation data were used together in calculating the biases and weights that form the ANN, and the test data set were completely independent for additional evaluation of model performance. The dates for training, validation and testing were randomly selected from the entire dataset for each training cycle.

The ANN networks were developed using feedforward networks with time delay and autoregressive networks (NARX, for Nonlinear Autoregressive Network with Exogenous Inputs). The ANN training used the back-propagation (Levenberg-Marquardt back-propagation) method for error minimization. For each model structure, the training was repeated until a correlation of >0.98 was obtained.

2.3 MODEL INPUT DATA

2.3.1 Flow

Flow data used in the ANN models were obtained from the DAYFLOW program (Rio Vista flow and Qwest flow are shown in Figure 2-2 and Figure 2-3). Because flow from Rio Vista is somewhat correlated to the Qwest flow (Figure 2-4), the Qwest flow can be expressed as residuals from real values and predicted values from the Rio Vista flow. The role of

freshwater flow in regulating salinity in the Delta was evaluated by using net Delta outflow alone, and with Rio Vista and Qwest flow as two separate terms in the training. A third alternative considered was the use of Qwest flow as a function of Rio Vista flow in the training with the residual as an additional input. The flow variables were evaluated using Models 1–3.

2.3.2 Tide

The role of tides was evaluated by using different numbers of tidal terms in the training, including three terms, two terms, one term, no tidal term, and by using the astronomical tide versus the actual tide (Models 4 to 8). Model performance in response to changes in the number of tidal terms was evaluated.

Hourly tide data are available from DWR for the San Francisco Golden Gate, Martinez, and Mallard Island locations. The ANN model used the difference between daily maximum and minimum tide, which represents tidal range as input at Golden Gate and Martinez. For Mallard Island, the average of daily minimum and daily maximum (half tide), which represents mean sea level, is used. Representative tide data from Golden Gate are shown in Figure 2-5.

The astronomical tide and the actual tide at Golden Gate used in the training were obtained from NOAA (mean seal level, MSL at hourly time steps) and converted to daily average values. When using the astronomical tide, the tides can be expressed as the astronomical tides and residuals between the actual and the astronomical tides. The residuals between actual tide and the astronomical tide were found to be a function of air pressure (Figure 2-6). Residuals between the actual and astronomical tides were not found to be correlated to other meteorological variables and are examined in Appendix A.

2.3.3 Salinity

The salinity data (EC, uS/cm) used in the training was obtained from CDEC, IEP, and STORET for a number of stations, which were then cleaned and filled. The data cleaning was done based on expected relationships between EC and flow at different locations such as those described in the G-model, and expected correlations between the adjacent stations. These expected functions were used to identify potential data errors in the dataset that were outside a certain range of the expected functions (e.g., two standard errors). The data cleaning procedures are described in Roy et al. (2013). The data filling was done using linear interpolation for data gaps less than 8 days. For data gaps that are more than 8 days, correlations with nearby stations were used to fill the gaps.

The data obtained from the USGS for stations in the Bay were for salinity in practical salinity units (psu). To be consistent with the EC data in $\mu\text{S}/\text{cm}$, the salinity data from USGS were converted to EC using the approach outlined by Schemel (2001).

$$X_{25,S} = \left(\frac{S}{35}\right) \times (53087) + S(S - 35) \times [J_1 + (J_2 \times S^{\frac{1}{2}}) + (J_3 \times S) + (J_4 \times S^{\frac{3}{2}})] \quad (1)$$

Where,

$$X_{25,S} = \text{EC at } 25^{\circ}\text{C}, J_1 = -16.072, J_2 = 4.1495, J_3 = -0.5345, J_4 = 0.0261.$$

Similar to the CDEC data, correlations between adjacent stations were used to fill larger data gaps (> 8 days). The salinity data obtained from the USGS for stations in the Bay included Point San Pablo (PSP) at near-surface and Carquinez (CAR) at mid-depth. The CAR station did not have measurements at near-surface depths. Previous studies have shown that no single and straight-forward relationship exists between bottom and surface salinity across multiple Bay stations (List, 1994), therefore a conversion from mid-depth and surface salinity (at a different location) was not performed for CAR. The data obtained at mid-depth for CAR were used directly in the training. Data from representative stations are shown in Figure 2-7 to Figure 2-10. Correlations used to fill data gaps in the CDEC data and the Bay stations are shown in Appendix B and C.

The filling procedures applied here to the cleaned daily salinity data resulted in a continuous block of salinity data from October 1974 to June 2012 for the Western Delta stations, and from September 1990 to September 2008 for the Bay stations. The Bay station records could not be extended further back in time because of the lack of continuous salinity data at suitable stations. In general, the quantity of continuous salinity data in the Bay is more limited than in the Western Delta stations, which have been used for compliance with water quality standards over many years.

2.3.4 Channel Depth

The role of channel depth was evaluated by training with and without the channel depth term, and comparing the results. Channel depth data are available from CDFG on monthly time intervals (Figure 2-11). In the analysis performed here, average water depth from channel locations in Suisun Bay (500s stations, <514) and Carquinez Strait (400s stations, <414) was used. For the training with depth, the length of the dataset is limited by the period of record of channel depth data (from 1978 onwards). Therefore, training with depth had fewer data points (~12,170 points) compared to training without channel depth as input (~13,770 points).

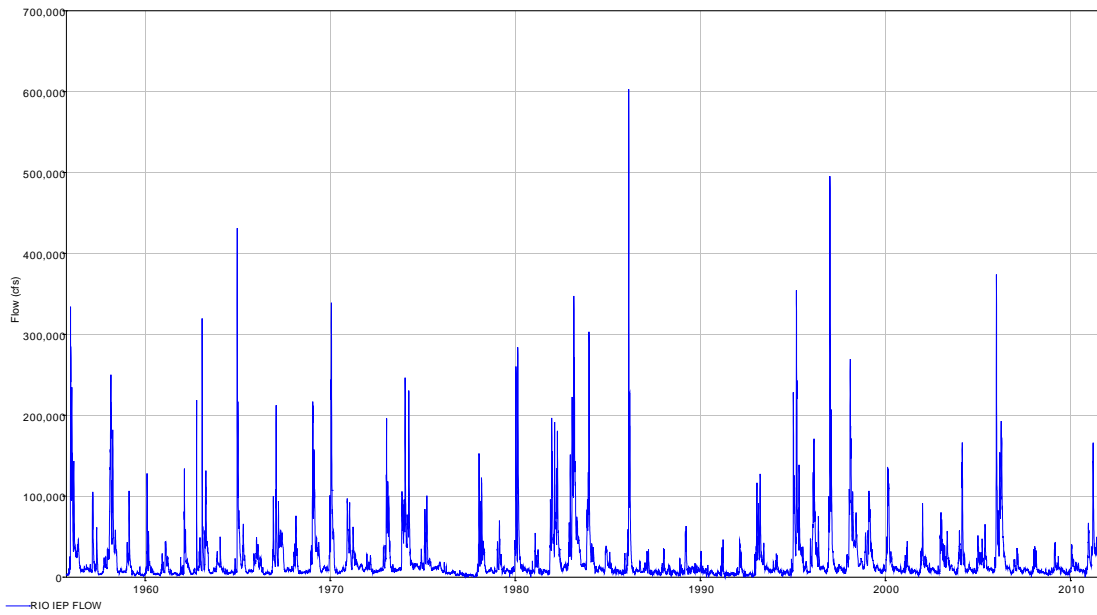


Figure 2-2 Daily Rio Vista flow from IEP DAYFLOW.

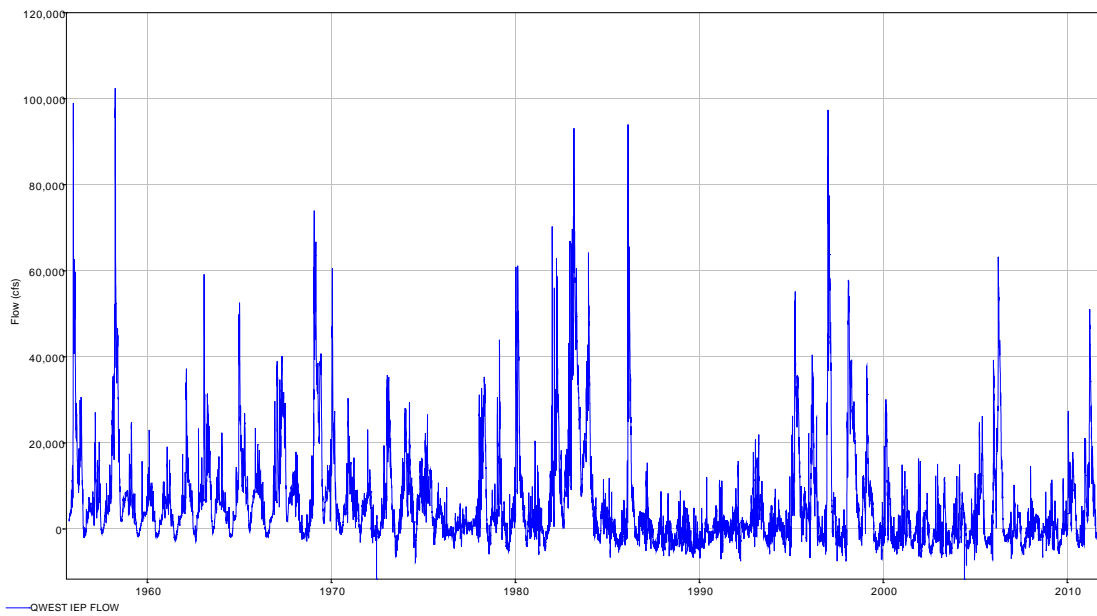


Figure 2-3 Daily Qwest flow from IEP DAYFLOW.

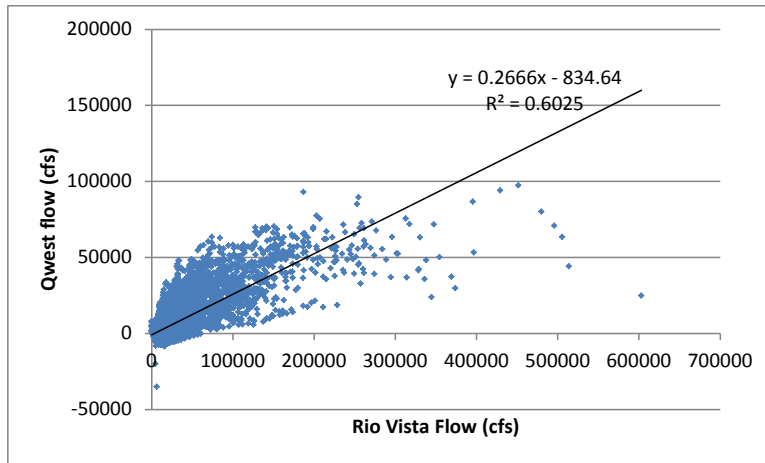


Figure 2-4 Correlation between Rio Vista flow and Qwest flow.

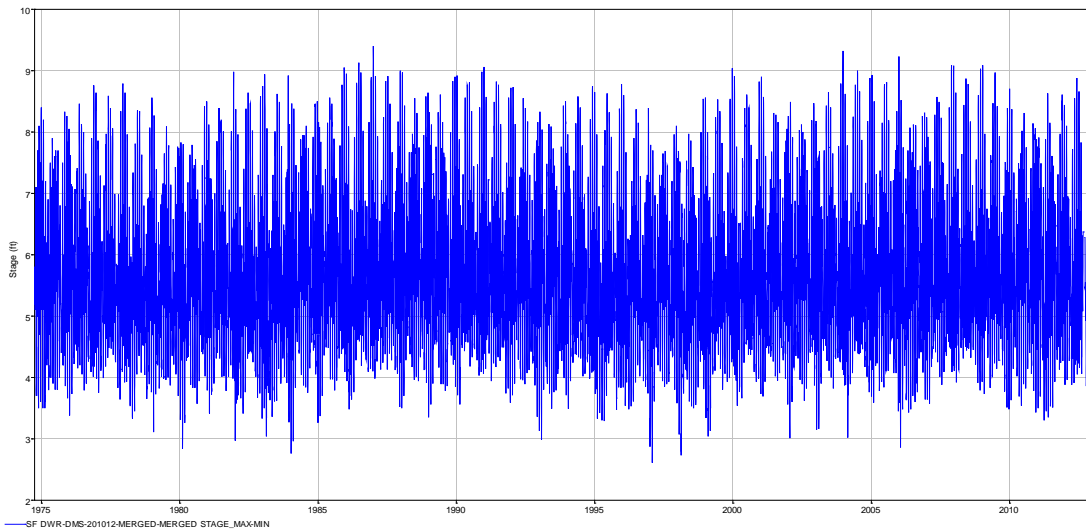


Figure 2-5 Tidal Range at Golden Gate.

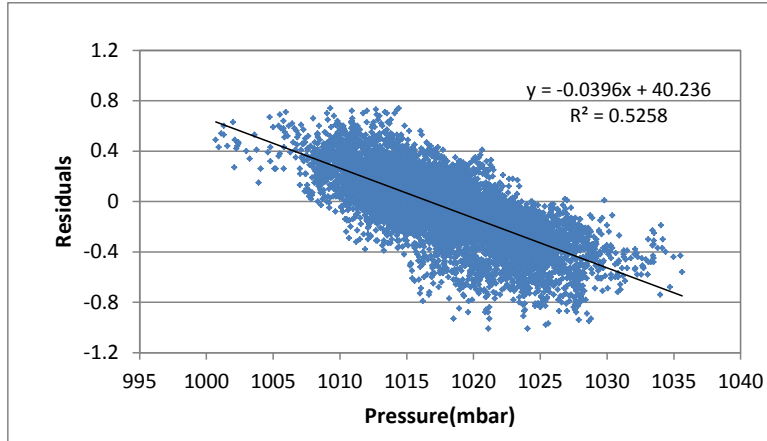


Figure 2-6 Correlation between residuals (difference between actual tide and astronomical tide) and air pressure at Golden Gate (Data source: NOAA).

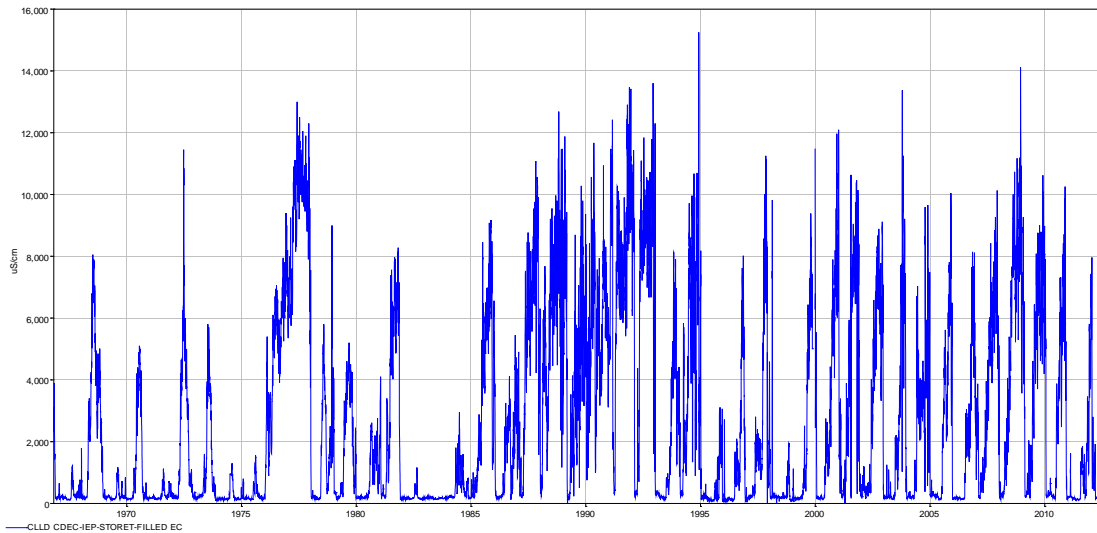


Figure 2-7 Cleaned and filled EC data at Collinsville (CLL).

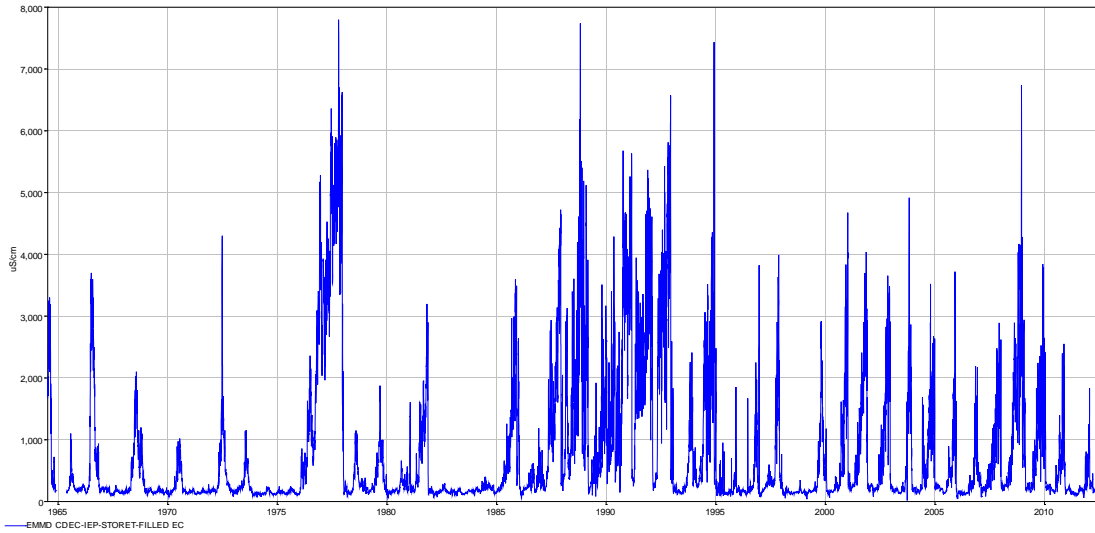


Figure 2-8 Cleaned and filled EC data at Emmaton (EMM).

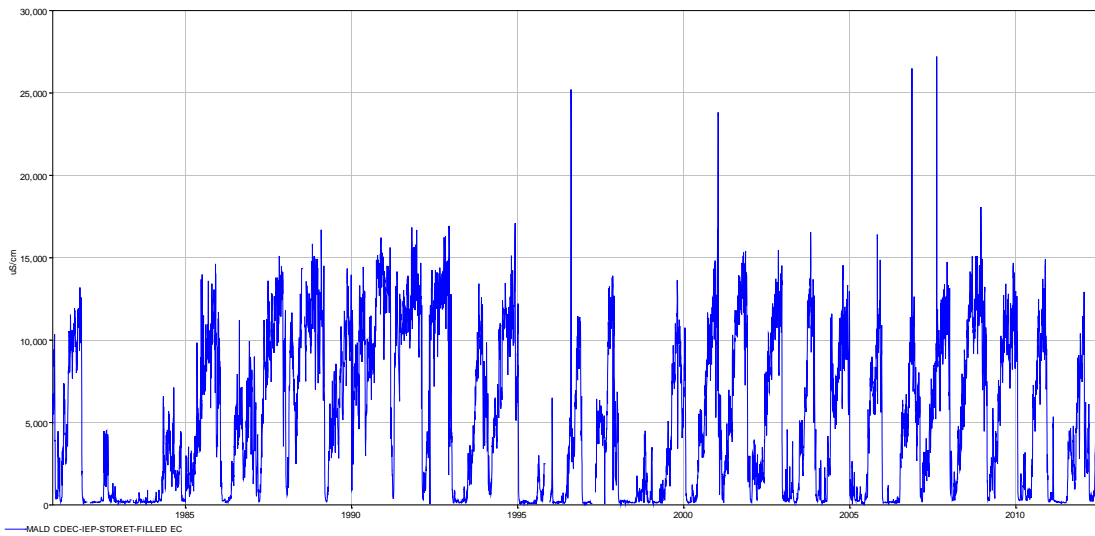


Figure 2-9 Cleaned and filled EC data at Mallard Island (MAL).

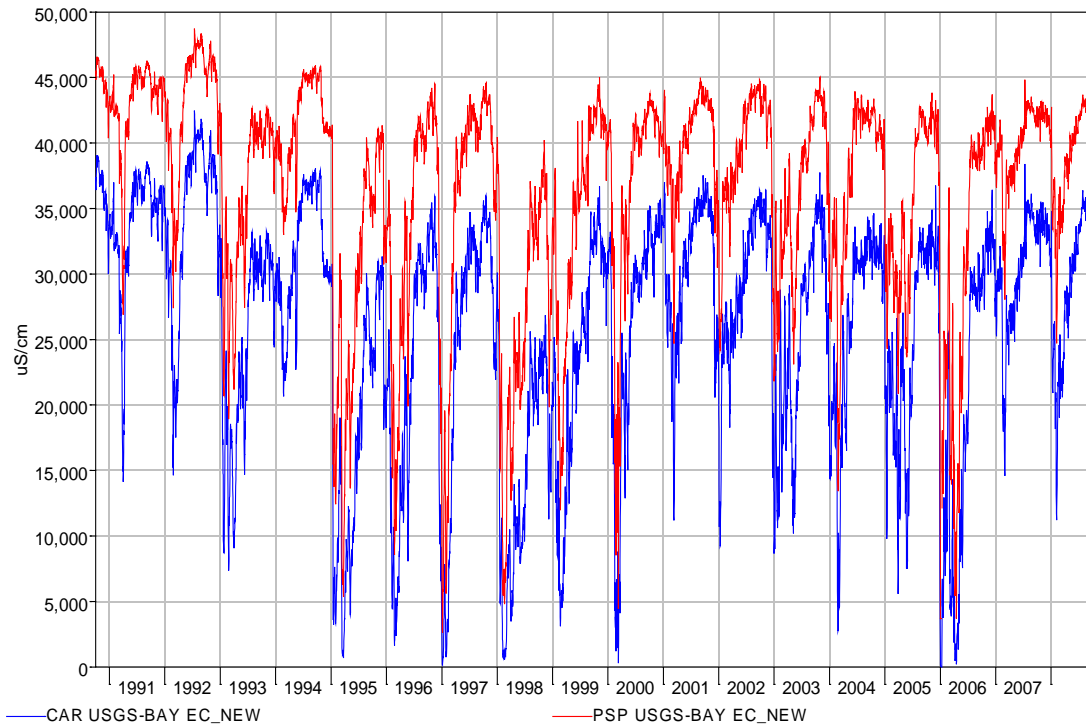


Figure 2-10 Cleaned and filled EC data at Carquinez (CAR) and Point San Pablo (PSP).

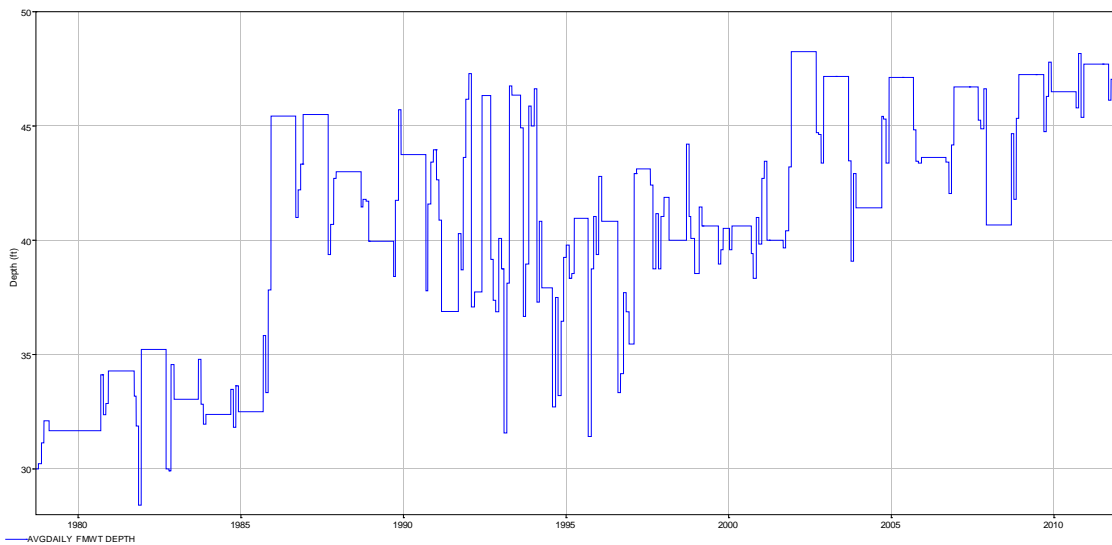


Figure 2-11 Channel Depth in Suisun Bay (Source: CDFG).

2.4 DESCRIPTION OF G-MODEL

The G-model was developed to predict salinity at specific locations in the Western Delta (Denton, 1993). Salinity at different locations is assumed to vary exponentially with outflow. Under similar outflow conditions, salinity levels can vary depending on flow over preceding time periods. Denton (1993) developed an equation that relates salinity to outflow and the antecedent flow to predict salinity at different locations. To take into account the flow history and the current salinity – flow relationship, an equation in the form of:

$$S(t) = (S_o - S_b)e^{-\alpha G(t)} + S_b \quad (2)$$

was developed, where S is salinity, α , S_o , and S_b are fitting parameters which vary with location, and $G(t)$ is a function of the antecedent outflow.

$G(t)$ is defined as:

$$\frac{\partial G}{\partial t} = \frac{(Q-G)G}{\beta} \quad (3)$$

It was suggested that the parameter β/G governs the rate at which G approaches its steady-state (i.e., the response of the estuary to changes in outflow will be slowest at low antecedent outflow G). Parameters for α , S_o , S_b and β have been calibrated for several stations in the Delta including Port Chicago, Chipps Island, Collinsville, and Jersey Point. Results of ANN simulations at specific locations were compared to the G-model calculations.

2.5 DESCRIPTION OF K-M MODEL

Kimmerer and Monismith (1992) developed an autoregressive equation that relates monthly values of X2 (in units of km from Golden Gate) with the net Delta outflow (NDO, in cfs) and the previous month's X2:

$$\text{Monthly X2}(t) = 122.2 + 0.3278 * \text{X2}(t-1) - 17.65 * \log_{10}(\text{NDO}(t)) \quad (4)$$

Computed values of X2 from the trained ANNs were compared to the K-M model calculations.

2.6 DSM-2 MODEL

DSM2 is a one-dimensional mathematical model for dynamic simulation of tidal hydraulics, water quality, and particle tracking in a network of riverine or estuarine channels. DSM2 can calculate stages, flows, velocities, transport of individual particles, and mass transport processes for conservative and non-conservative constituents. DSM-2 has been used extensively by DWR's Delta Modeling Section for various applications related to flow and water quality in the Delta, and specifically for simulating EC over the 1990-2010 period (Sandhu, N., 2011, personal communication). In this work, DSM-2 computed values of salinity at individual locations and X2 values interpolated from fixed station salinity values were compared to ANN calculations.

3. RESULTS

This chapter presents the results of the ANN training, comparison to existing predictive models of salinity in the Delta (the G-model, K-M model, and DSM-2), sensitivity to changes in flow, sea level, and air pressure, and comparison with historical salinity data observed prior to the training period, spanning 1929-1971.

3.1 ANN NETWORK TRAINING RESULTS

Results of the ANN training for different models (10 models, as defined in Table 2-1) are summarized in Table 3-1 to Table 3-6, by computing the correlation (R) between outputs and observed values at distances corresponding to fixed stations. Model outputs are compared to observations in time-series form and scatterplots in the attached Appendix D.

3.1.1 *Flow Variables*

The influence of flow was evaluated by comparing models that included net Delta outflow only, Rio Vista and Qwest flow, and Rio Vista flow and Qwest expressed as function of Rio Vista flow. The definitions of the models evaluated for flow (Models 1-3) are shown in Table 2-1. The results show clearly improved model results by including two flow terms versus the net Delta outflow term, especially for the Sacramento River stations (Table 3-1). Changing flow inputs to either Rio Vista and Qwest flow as separate variables or to Qwest flow as a function of Rio Vista gave similar results, with slightly poorer fits for the Sacramento River model but slightly improved fits for the San Joaquin River model. For the purpose of this evaluation, both alternatives are considered equally valid, and Models 2 and 3 are both acceptable. Going forward, Model 3 is used for comparison and additional evaluation of different inputs.

Table 3-1
Comparison of Observations and ANN Model Outputs (R) for Evaluating Flow Terms

	Model 1: 1 Flow Model (Delta Outflow)	Model 2: 2 Flow Model (Rio Vista, Qwest)	Model 3: 2 Flow Model (Rio Vista, residuals for Qwest)
Sacramento River			
PSP	0.949	0.976	0.965
CAR	0.964	0.976	0.975
MRZ	0.949	0.963	0.962
PCT	0.930	0.951	0.949
MAL	0.911	0.941	0.940
CLL	0.852	0.938	0.933
EMM	0.749	0.881	0.868
SDI	0.808	0.880	0.861
RVB	0.457	0.648	0.490
San Joaquin River			
PSP	0.960	0.960	0.966
CAR	0.969	0.973	0.975
MRZ	0.959	0.960	0.961
PCT	0.947	0.949	0.951
MAL	0.940	0.939	0.938
PTS	0.879	0.882	0.883
ANH	0.927	0.933	0.933
BLP	0.863	0.868	0.871
JER	0.859	0.850	0.861
TSL	0.807	0.706	0.810
SAL	0.485	0.428	0.496

3.1.2 Tide Variables

The roles of tide variables were evaluated by decreasing tidal terms from three terms to two terms, one term, no tidal term and using the actual and astronomical tide. Definitions of models evaluated relating to tidal terms (Models 3 to 8) are shown in Table 2-1. Training results show that decreasing tidal terms does not result in significant degradation in the training results (Table 3-2, and attached Appendix D showing scatterplots and time series plots at fixed locations). Therefore, relatively good training results can be achieved by using just one tidal term. Some degradation was seen for the Sacramento River model when inputs were decreased from one tide to no tide. This suggested that including one tidal term in the training is beneficial. The astronomical tide (plus a residual term for actual tide) was found to be as good as or better than using the actual tide terms, recommending the use of the astronomical tide approach because of its easier predictability. During the use of the

ANN models in a predictive mode, the residual between the astronomical tide and actual tide can be estimated using the pressure-residual correlation presented earlier.

**Table 3-2
Comparison of Models Regarding Tide (R)**

	Model 3: Astronomical Tide plus residual	Model 4: 3 Tides	Model 5: 2 Tides	Model 6: 1 Tide (Golden Gate Range)	Model 7: No tide	Model 8: 1 Tide (Golden Gate MSL)
Sacramento River						
PSP	0.965	0.957	0.949	0.959	0.939	0.971
CAR	0.975	0.970	0.972	0.973	0.961	0.972
MRZ	0.962	0.956	0.955	0.957	0.942	0.957
PCT	0.949	0.948	0.942	0.944	0.930	0.943
MAL	0.940	0.930	0.931	0.923	0.912	0.928
CLL	0.933	0.930	0.927	0.927	0.894	0.926
EMM	0.868	0.880	0.860	0.867	0.815	0.865
SDI	0.861	0.877	0.861	0.863	0.818	0.862
RVB	0.490	0.642	0.643	0.623	0.562	0.678
San Joaquin River						
PSP	0.966	0.949	0.966	0.955	0.964	0.950
CAR	0.975	0.965	0.974	0.962	0.971	0.964
MRZ	0.961	0.951	0.958	0.951	0.952	0.950
PCT	0.951	0.940	0.947	0.923	0.937	0.937
MAL	0.938	0.927	0.931	0.903	0.918	0.924
PTS	0.883	0.872	0.877	0.844	0.866	0.861
ANH	0.933	0.915	0.924	0.860	0.905	0.903
BLP	0.871	0.856	0.852	0.797	0.841	0.838
JER	0.861	0.852	0.856	0.786	0.845	0.822
TSL	0.810	0.824	0.767	0.749	0.815	0.799
SAL	0.496	0.610	0.519	0.514	0.669	0.568

3.1.3 Antecedent Salinity Input

The results show that including the antecedent salinity values as inputs improved the training results (Models 9 and 10; results in Table 3-3 and Appendix D). The change was significant at the eastern stations along both rivers (EMM, RVB, SDI, JER, BLP, PTS, and SAL). These interior stations have lower salinities than the remaining fixed stations evaluated, are likely to have longer flushing times, and are more influenced by flows from the watershed.

These models illustrate the benefit of using antecedent salinity to improve fits at specific locations, although it is noted that the input requirements are more complex. In particular, for predictions performed over long durations, the antecedent salinity is unknown and must

be estimated using the ANN resulting in potential errors. An alternative approach, presented below, is the use of station-specific ANNs to improve fits at selected locations that are considered important from the standpoint of compliance.

**Table 3-3
Comparison of Models on Antecedent salinity Input (R)**

	Model 3: FFW	Model 9: Previous 30-day Salinity Input	Model 10: NARX
Sacramento River			
PSP	0.965	0.982	0.989
CAR	0.975	0.982	0.993
MRZ	0.962	0.988	0.990
PCT	0.949	0.987	0.988
MAL	0.940	0.987	0.988
CLL	0.933	0.984	0.984
EMM	0.868	0.964	0.947
SDI	0.861	0.955	0.931
RVB	0.490	0.642	0.549
San Joaquin River			
PSP	0.966	0.982	0.995
CAR	0.975	0.984	0.995
MRZ	0.961	0.989	0.992
PCT	0.951	0.988	0.991
MAL	0.938	0.988	0.991
PTS	0.883	0.982	0.983
ANH	0.933	0.985	0.990
BLP	0.871	0.976	0.982
JER	0.861	0.972	0.988
TSL	0.810	0.956	0.982
SAL	0.496	0.560	0.796

3.1.4 Overall Model Performance

Excluding the models with antecedent salinity input, the best models are Model 2 (using astronomical tide, and Rio Vista and Qwest flow as two separate input variables) and Model 3 (astronomical tide, and Rio Vista flow and Qwest flow as function of Rio Vista). The model using Golden Gate mean sea level, Rio Vista flow and Qwest flow as function of Rio Vista flow (Model 8) also has relatively good performance.

Table 3-4 shows the performance (R^2 and standard error, SE) of a trained model (Model 3) at different locations for daily values and monthly averages. The monthly averages were not

developed from a separate model; the daily data were aggregated to a monthly level for comparison. The results show R^2 values of 0.75–0.95 at different locations. Standard errors in the model ranged from 276–2,396 $\mu\text{S}/\text{cm}$ for daily values. The performance was lower at RVB, SAL and TSL. These stations generally have minimal oceanic influence, low EC values, and greater noise relative to the mean. These stations are more challenging to model in a distance-salinity framework where the Bay and Western Delta are included.

Table 3-4
Performance of Trained Salinity ANN Model (Model 3) at Different Locations
ANN Salinity (uS/cm) = $\Phi 1$ + $\Phi 2$ *Observed Salinity (uS/cm)

	Daily				Monthly			
	$\Phi 2$	$\Phi 1$	R ²	SE	$\Phi 2$	$\Phi 1$	R ²	SE
Sacramento River								
PSP	0.951	1750.4	0.932	2177.6	0.979	754.4	0.969	1393.3
CAR	0.988	318.5	0.952	2078.4	1.014	-355.5	0.981	1264.9
MRZ	0.908	1542.0	0.925	2323.6	0.933	1115.6	0.949	1832.0
PCT	0.872	1288.7	0.901	2096.5	0.901	984.8	0.939	1581.5
MAL	0.917	664.1	0.885	1466.4	0.939	549.9	0.915	1202.6
CLL	0.795	468.3	0.876	948.4	0.819	396.9	0.920	723.5
EMM	0.828	137.7	0.788	487.1	0.877	95.2	0.889	326.2
SDI	0.946	82.7	0.780	451.9	1.002	41.6	0.894	287.7
RVB	1.458	82.4	0.295	409.7	1.581	53.0	0.563	234.9
San Joaquin River								
PSP	0.9384	2294.0	0.934	2114.9	0.967	1233.5	0.975	1251.2
CAR	0.9977	-29.4	0.950	2125.1	1.019	-580.2	0.981	1269.0
MRZ	0.9041	1635.3	0.924	2329.7	0.929	1208.3	0.950	1811.4
PCT	0.8827	1158.5	0.904	2088.4	0.914	829.1	0.943	1538.1
MAL	0.9319	815.8	0.879	1528.5	0.956	689.4	0.912	1246.3
PTS	0.6837	883.0	0.780	1592.3	0.715	737.5	0.835	1316.6
ANH	0.9265	318.5	0.871	730.2	0.952	268.9	0.921	543.7
BLP	0.9516	67.5	0.759	564.3	1.006	11.3	0.856	409.1
JER	1.0512	-48.3	0.742	435.1	1.088	-74.9	0.855	301.0
TSL	0.9910	-61.2	0.656	369.0	1.037	-85.7	0.822	236.2
SAL	1.7296	-153.3	0.246	332.9	2.018	-219.0	0.483	210.7

3.1.5 Time Delay

The increase of time delay from 30 days to 60 days for a representative model (Model 6 for the Sacramento River in Table 2-1) showed some improvements at selected stations but showed decreases at other stations (Table 3-5). There is slight improvement in overall performance as the time delay is increased from 30 days to 60 days, however, the net improvement was not considered large enough given the significant additional computational time for ANN training. Furthermore, the distance-salinity framework, even with the longer delay, does not address the issues of poorer performance at eastern stations such as EMM, RVB, and SDI. Given these reasons, the 30-day time delay was retained for the distance-salinity ANNs.

**Table 3-5
Comparison of Training Results with Different Time Delays (R)**

	30 Days Delay (Using 1 Tide term)	60 Days Delay (Using 1 Tide term)
Sacramento River		
PSP	0.928	0.948
CAR	0.942	0.951
MRZ	0.955	0.958
PCT	0.942	0.946
MAL	0.883	0.931
CLL	0.925	0.929
EMM	0.870	0.851
SDI	0.872	0.856
RVB	0.633	0.613
Overall	0.982	0.986

3.1.6 Channel Depth

The effect of channel depth was evaluated by performing training with and without the depth term. As noted in chapter 2, this was done as part of the initial screening. Results are shown in Table 3-6 for a set of models (identified as A through G to distinguish from the final set of candidate models in Table 2-1). The results demonstrate that training with or without channel depth does not affect the quality of the fits significantly or in a systematic manner. Following the initial screening the depth effect was explored by adding this input to Model 3, previously identified as a suitable model for salinity prediction. The results are shown in Table 3-7 and Appendix E, and are consistent with Table 3-6. Based on these reasons, depth was not included in the recommended models. It is important to note however, that there may be a depth effect on salinity, only that it may have been overwhelmed by the flow- and tide-induced variability over daily time scales.

Table 3-6
Comparison of Training Results With and Without Consideration of Depth

Model	Tidal Terms	Time Lag	Sacramento River Model	Sacramento River Model	San Joaquin River Model	San Joaquin River Model
			r (without depth)	r (with depth)	r (without depth)	r (with depth)
A	3	7	0.981	0.981	0.980	0.982
B	2	7	0.981	0.982	0.980	0.979
C	1	7	0.979	0.981	0.978	0.979
D	1	30	0.982	0.984	0.985	0.983
E	No tide	7	0.949	0.956	0.877	0.967
F	Astronomical tide	7	0.981	0.997	0.996	0.979
G	Astronomical tide	30	0.983	0.985	0.985	0.983

Table 3-7
Comparison of Channel Depth Effects Added to Model 3

	Model 3: No depth term	Model 3: With depth term
Sacramento River		
PSP	0.965	0.951
CAR	0.975	0.956
MRZ	0.962	0.961
PCT	0.949	0.944
MAL	0.940	0.955
CLL	0.933	0.927
EMM	0.868	0.836
SDI	0.861	0.841
RVB	0.490	0.604
San Joaquin River		
PSP	0.966	0.941
CAR	0.975	0.951
MRZ	0.961	0.961
PCT	0.951	0.942
MAL	0.938	0.954
PTS	0.883	0.867
ANH	0.933	0.917
BLP	0.871	0.829
JER	0.861	0.818
TSL	0.810	0.763

SAL	0.496	0.441
-----	-------	-------

3.2 COMPARISON OF RESULTS TO G-MODEL

The results of using the G-model in the predictions of salinity at selected locations (CLL, PCT, and JER) are shown in Figure 3-1 through Figure 3-3. Overall, the G-model does well at describing the data at these locations, with poorer fits at the more inland JER location. The performance of the ANN models compared to G-model at these locations is better for CLL and PCT, except model 7 with no tide input (Table 3-8). The comparison at JER showed mixed results, with ANNs doing as well as or slightly poorer than the G-model. It is noted that the ANN model is trying to capture salinity at all locations in the Bay and Sacramento and San Joaquin Rivers with two models, predicting salinity at different locations based on distance. Therefore, the performance at individual locations may be lower, as compared to the G-model that was tuned on a site-specific basis.

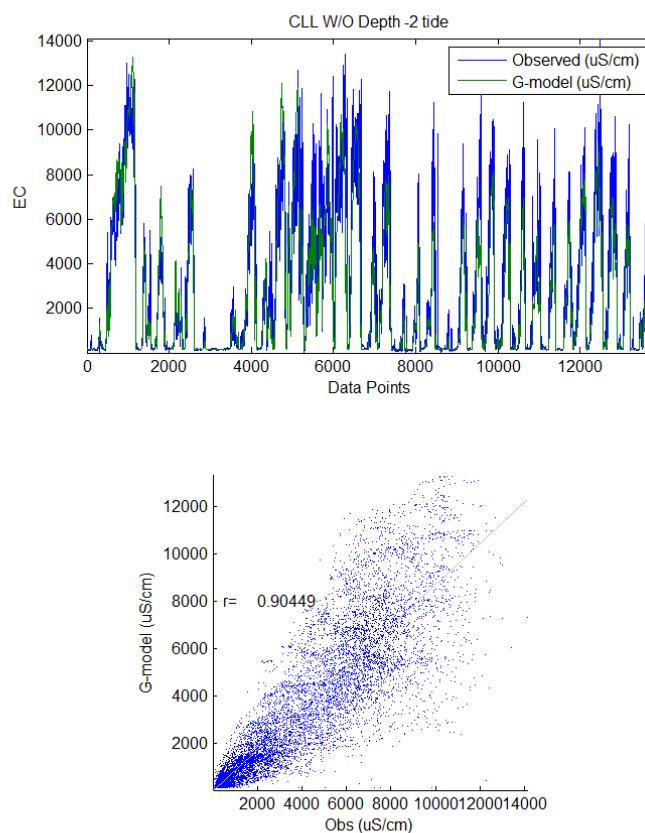


Figure 3-1 G-model performance at Collinsville (CLL).

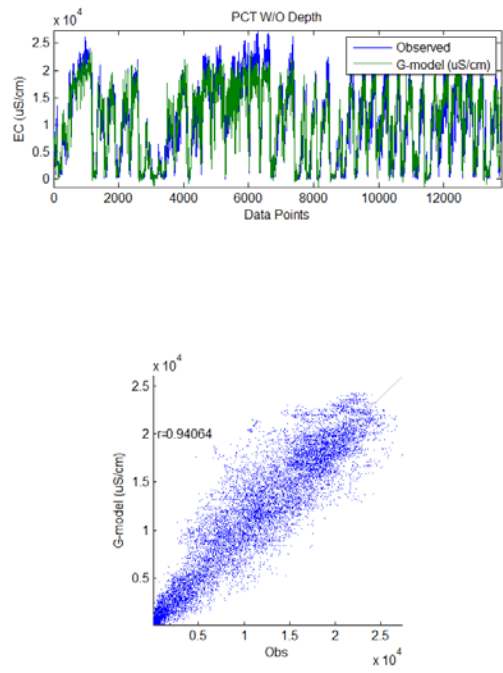


Figure 3-2 G-model performance at Port Chicago (PCT).

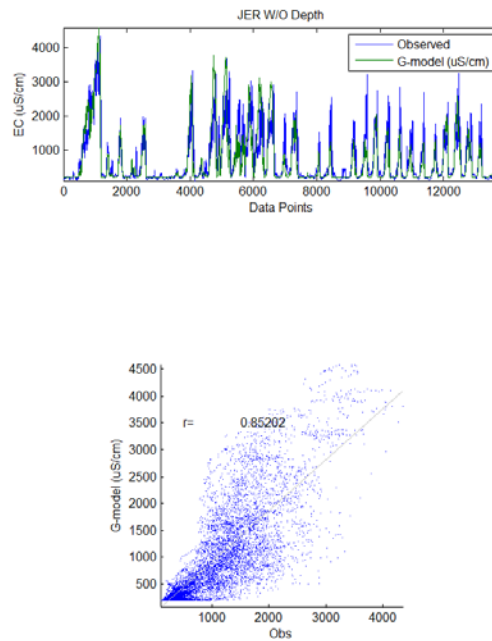


Figure 3-3 G-model performance at Jersey Point (JER).

Table 3-8
Comparison of Model Performance to G-model

Model	CLL	PCT	JER
1	0.927	0.944	0.808
2	0.938	0.951	0.850
3	0.933	0.949	0.861
4	0.930	0.948	0.852
5	0.927	0.942	0.856
6	0.927	0.944	0.786
7	0.894	0.930	0.845
8	0.926	0.943	0.822
9	0.984	0.987	0.972
10	0.984	0.988	0.988
G-model	0.904	0.941	0.852

3.3 ANN MODELS FOR SPECIFIC STATIONS

Four representative stations, PCT, CLL, EMM and JER, were considered for the development of station-specific ANNs. As noted above, salinity at some of these stations is not predicted as well by the feedforward models, notably EMM and JER. In this exercise, similar flow and tide inputs were used as for the distance-salinity ANNs, however, distance was not an input, and there was a single output: the salinity at the desired location. Furthermore, the time delay was also increased to explore whether this results in an improvement in fit for these locations (as opposed to an improvement in the general salinity-distance models). In Table 3-9, results from this exercise are compared to the distance-salinity models (Models 2 and 9 in Table 2-1) and the fits obtained from the G-Model. For the eastern stations (EMM and JER), there is an improvement in fits using the single station feedforward models versus the distance-salinity models, and the fits are better than for the G-model. There is also a small improvement in fit when a longer time delay (60 days versus 30 days) is considered. Notably, the improvement in fit with respect to time delay is greater for the more eastern stations (CLL, EMM, JER) than for the station closest to Golden Gate (PCT). This may explain why the time delay beyond 30 days was not found to be significant in the training for the overall distance-salinity relationship, which contains several stations that are west of CLL. Although the fits from the single-station models are not as good as the model using antecedent salinity (Model 9), they are based on boundary inputs alone (flow, tides), and, for long forecast periods, easier to use than models that require knowledge of antecedent salinity.

Table 3-9
Comparison of Selected Distance-Salinity ANN Models, Station-Specific ANN models, and G-model

Model	PCT	CLL	EMM	JER
Model 3, Distance-Salinity	0.949	0.936	0.888	0.861
Model 9, Distance-Salinity	0.987	0.984	0.964	0.972
Single station model (30 day delay)	0.953	0.954	0.951	0.945
Single Station Model (60 day delay)	0.960	0.967	0.961	0.967
G-model	0.941	0.904	N/A	0.852

3.4 USE OF TRAINED NETWORK IN X2 CALCULATIONS

The trained networks can be used to estimate X2 locations based on the calculated salinity at specific output locations, using the 2-point method in Kimmerer and Monismith (1992), using log salinity versus linear distance for interpolation. The results of X2 calculations from Model 3 were compared to X2 derived from the observed data (or “observed X2”) in Figure 3-4 for the Sacramento River model and Figure 3-5 for the San Joaquin River model. X2 values from both the Sacramento River ANN model and the San Joaquin River ANN model showed very good agreement with the X2 derived from the observed data for the Sacramento River stations and the San Joaquin River stations ($R^2 = 0.9762$ and $R^2 = 0.9671$).

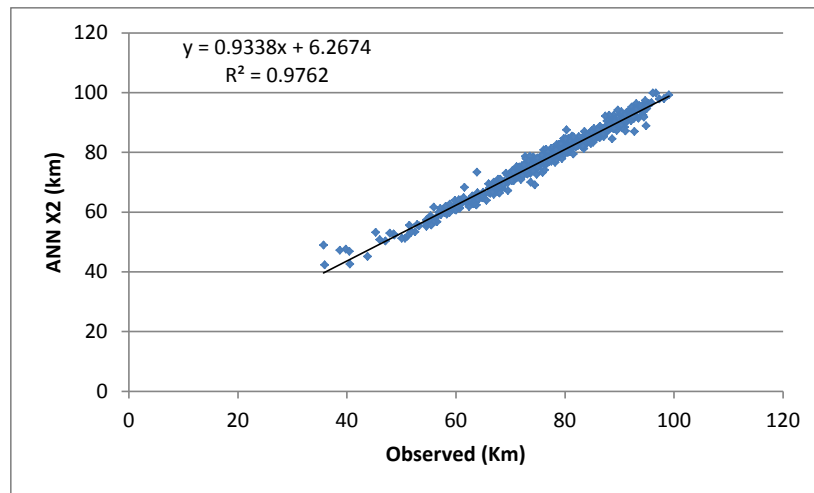
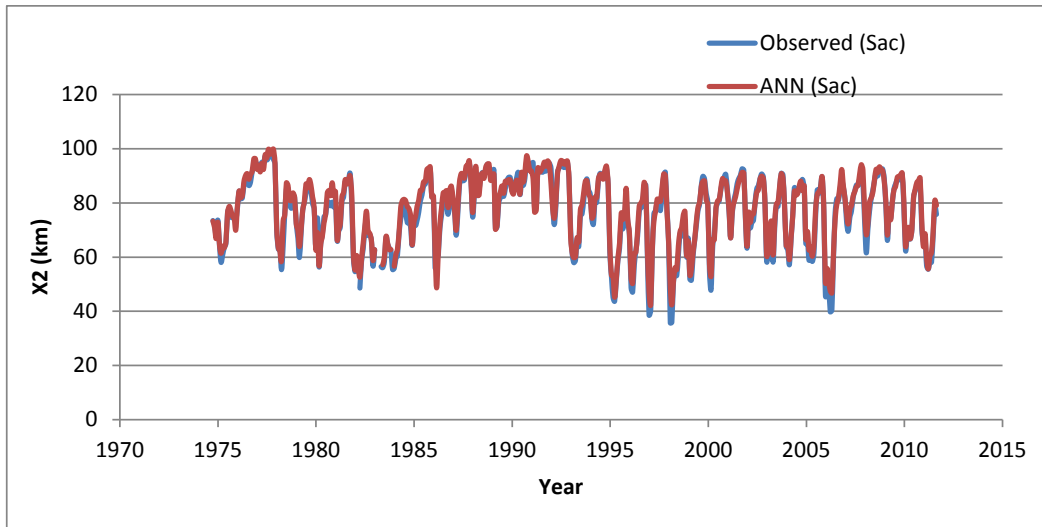


Figure 3-4 Comparison of X2 calculated from the ANN model and the observed X2 for the Sacramento River stations.

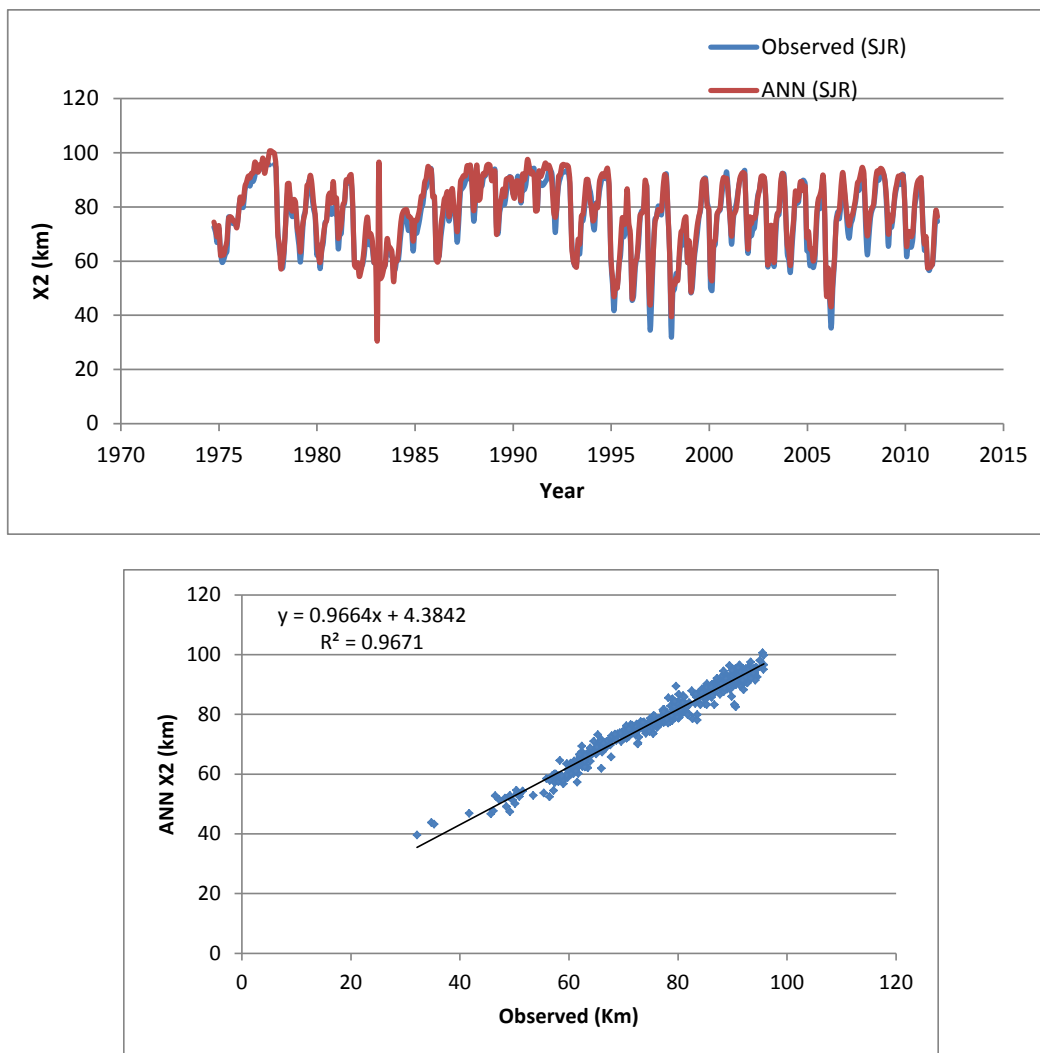


Figure 3-5 Comparison of X2 calculated from the ANN model to the observed X2 for the San Joaquin River stations.

3.5 COMPARISON TO K-M MODEL

The calculated X2 from the K-M model was compared to the observed X2 for the Sacramento River stations (Figure 3-6) and the San Joaquin River stations (Figure 3-7). The correlation between X2 from the K-M model and the observed X2 ($R^2 = 0.9212$ and $R^2 = 0.9068$) is lower than the correlation between the ANN model and the observed X2 reported in the previous section. Comparison of X2 from the ANN models and the K-M model suggested a pattern of slightly lower values from the K-M model (Figure 3-8).

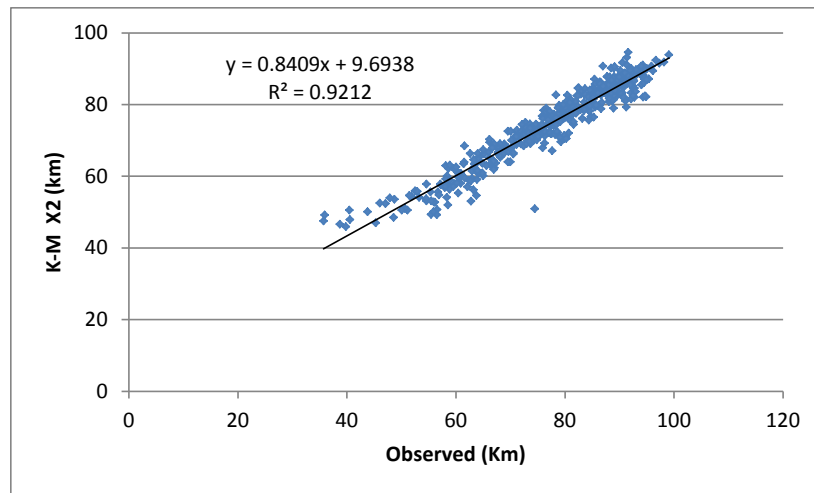
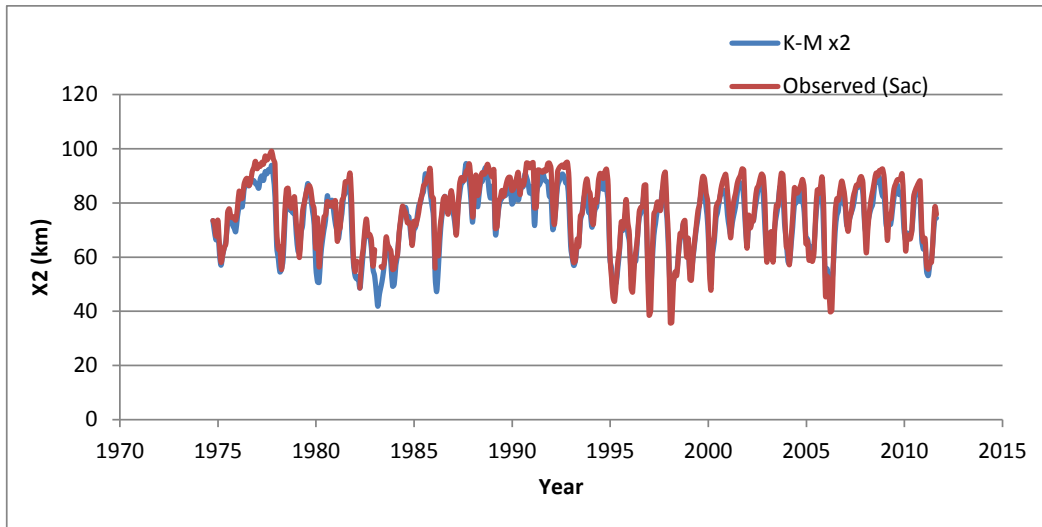


Figure 3-6 Comparison of X2 position calculated from K-M equation and the observed X2 for the Sacramento River stations.

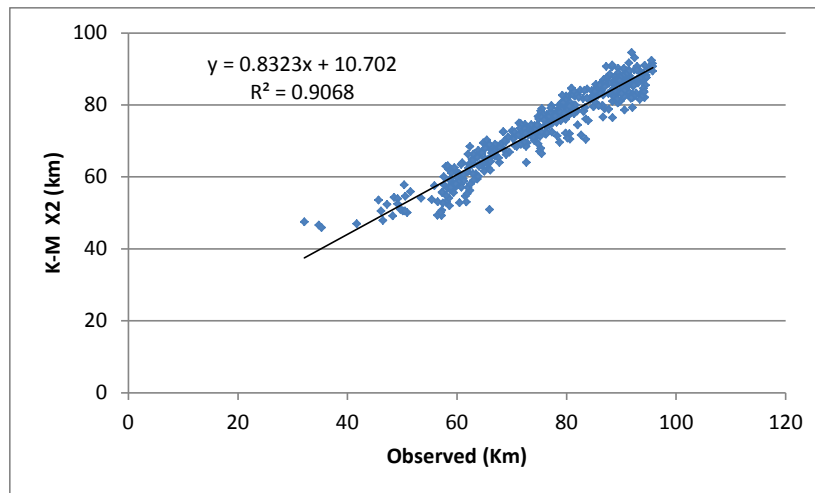
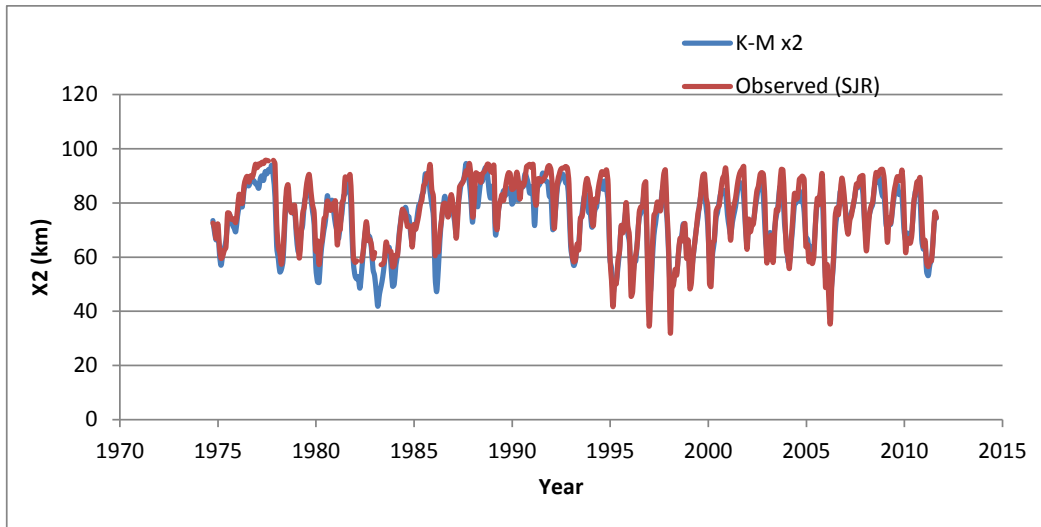


Figure 3-7 Comparison of X2 calculated from the K-M equation and the observed X2 for the San Joaquin River stations.

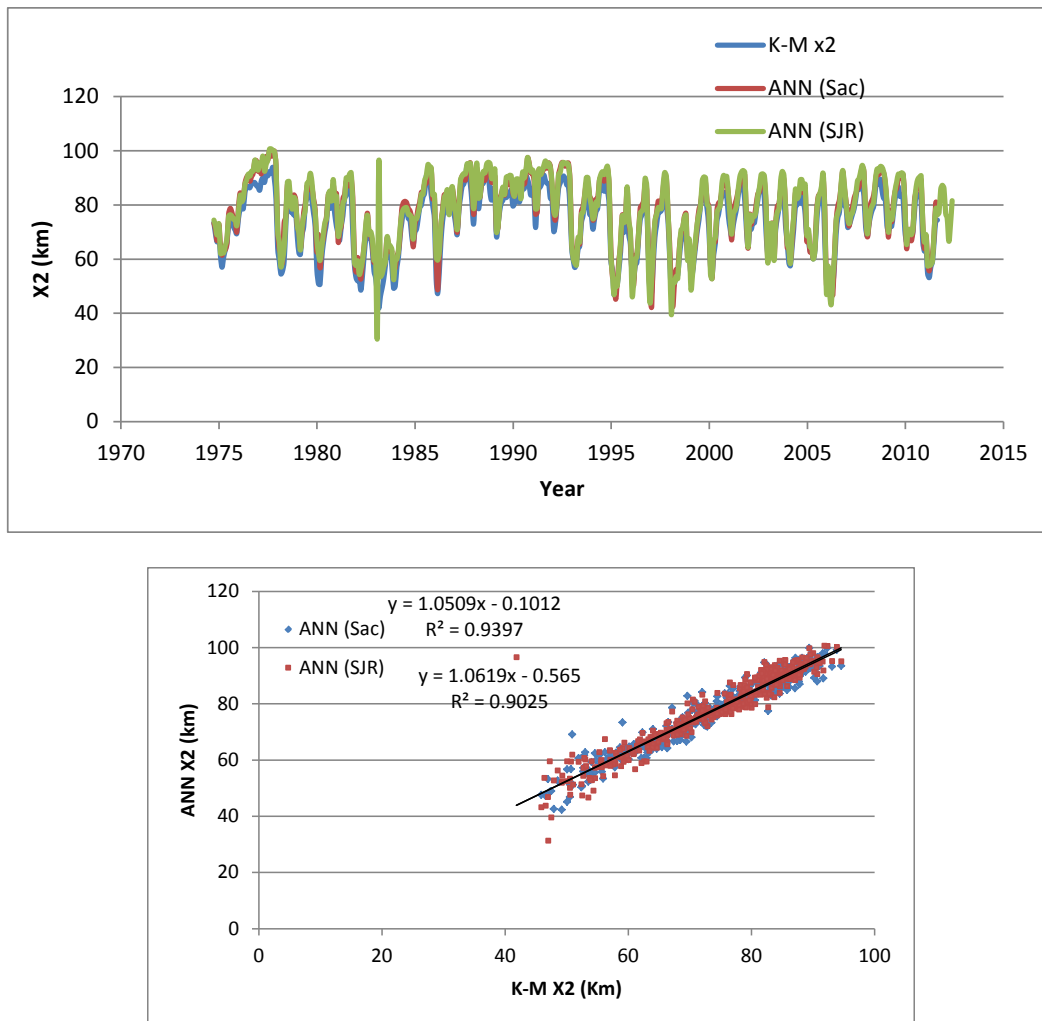


Figure 3-8 Comparison of X2 position calculated from K-M model to the ANN models for the Sacramento River and the San Joaquin River stations.

3.6 COMPARISON WITH DSM2 MODEL

Station-specific ANN model values of salinity (EMM and JER; with a 30-day delay) were compared to values obtained from the DSM2 model, run over the 1990-2010 period (Figure 3-9). The comparison shows that the station-specific ANNs provide a better fit to the data at these stations. As noted before, the JER station is also more challenging to fit using the G-model.

X2 values can be computed from DSM2 salinity values, as long as the values are east of Martinez (which forms the western boundary of the DSM2 model). A comparison of the DSM2-computed X2 values are compared to the observed X2 values in Figure 3-10 and Figure 3-11. The fits are reasonable, although not as good as those obtained for the ANN models (Figure 3-4 and Figure 3-5). The standard errors associated with the different X2 calculation approaches are shown in Table 3-10.

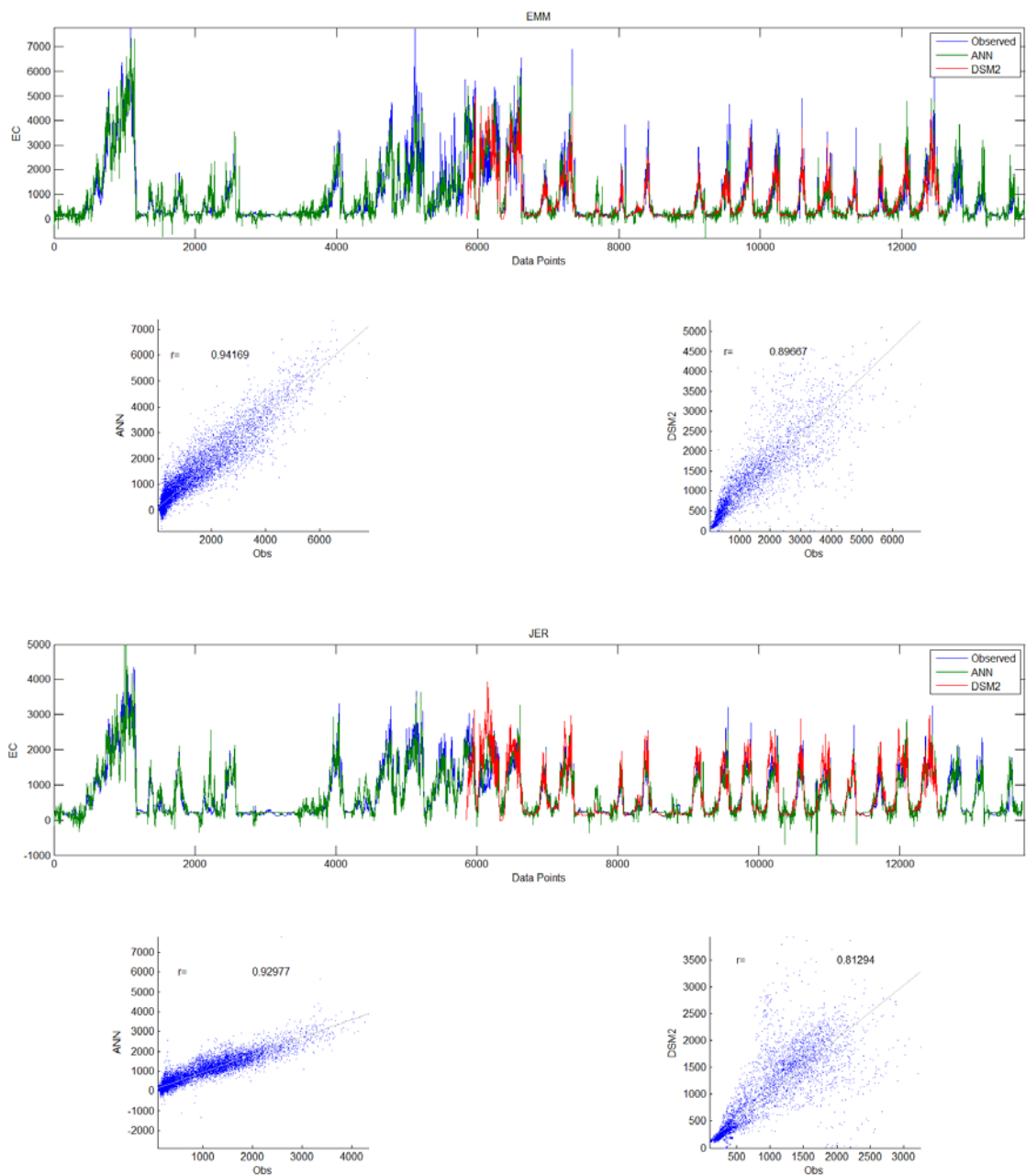


Figure 3-9 Comparison of observed daily salinity to values calculated by the DSM-2 and ANN models for the EMM and JER stations, shown as a time series (beginning October 1, 1974) and scatterplot. DSM-2 values were available for a 20-year period from 1990-2010.

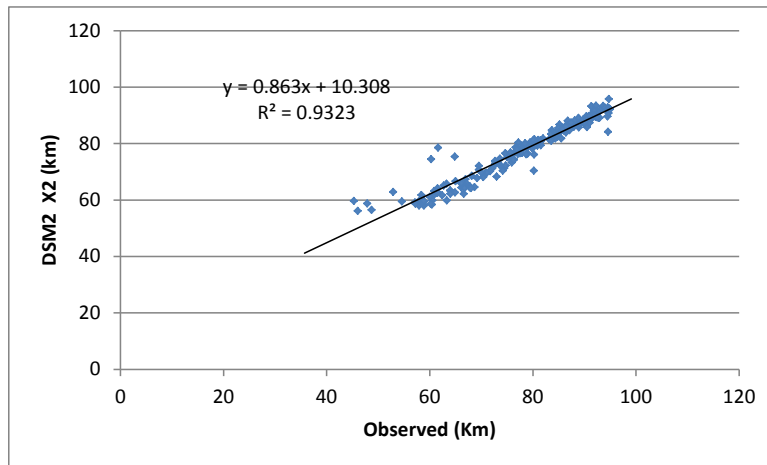
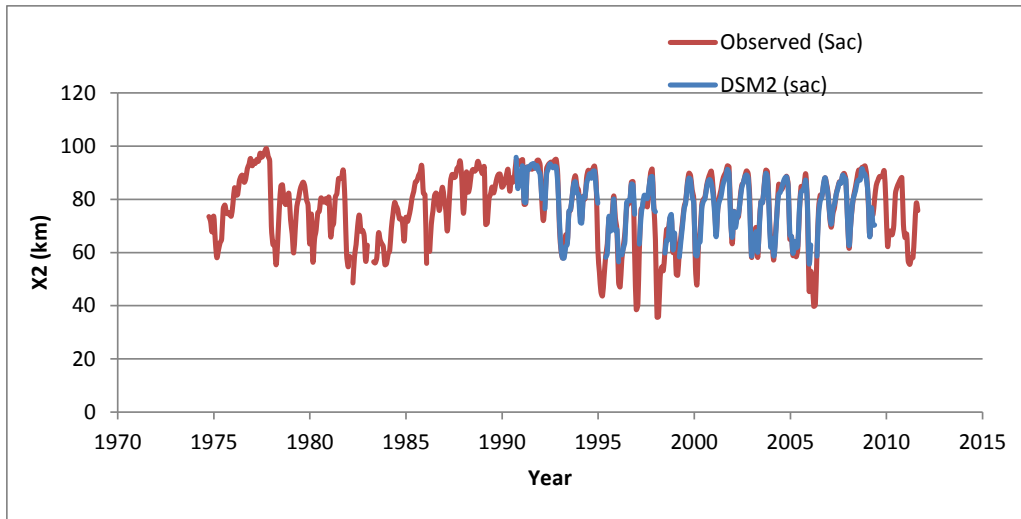


Figure 3-10 Comparison of X2 calculated from the DSM2 model to the observed X2 (Sacramento River).

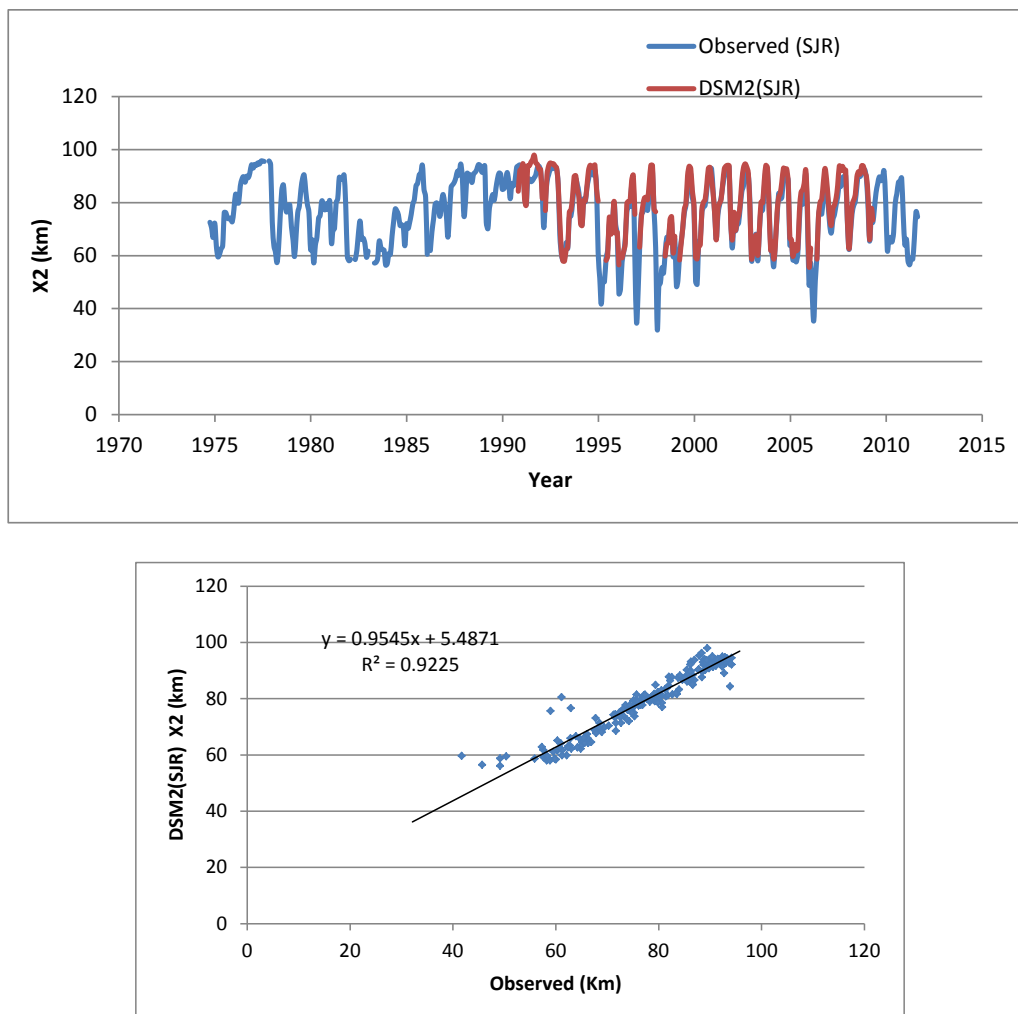


Figure 3-11 Comparison of X2 calculated from the DSM2 model to the observed X2 (San Joaquin River).

Table 3-10
Standard Error (km) Associated with X2 Estimation

Standard Error (km)	K-M Model	ANN Model	DSM2
Sacramento River	3.18	1.96	2.73
San Joaquin River	3.43	2.29	3.29

3.7 SENSITIVITY ANALYSIS AND CHANGES DUE TO SEA LEVEL RISE

A trained ANN (Model 3) was used to project EC over distance under different flow conditions from Rio Vista: 1,000, 5,000, 10,000, 25,000, and 50,000 cfs. For the sensitivity analysis, the inputs for the ANN model are: distance, Rio Vista flow, Qwest flow, astronomical tide, and the residuals between the actual and astronomical tide. The model

was run in steady state where the flow inputs were held constant at different values. The values for distance were specified at 10 km intervals. The Qwest flow was specified as a function of Rio Vista flow, using the function shown in Figure 2-4. The astronomical tide and tide residuals used were averages of the most recent 10 years (2002-2012). The results represent EC over distance under different flow conditions for a set condition of average tidal conditions. Simulated EC as a function of distance decreases from Golden Gate, with lower EC under higher flows (Figure 3-12). Following the presentation in Jassby et al. (1995), simulated EC values were plotted as a function of standardized distance (X/X_2). The approach results in different curves of “self-similarity” as Rio Vista flow increases (e.g., 25,000 cfs; Figure 3-12). Although not shown in this form, previous results have shown the changing of the horizontal salinity structure at higher Delta outflows (Monismith et al., 2002).

Sea level at Golden Gate Bridge has increased at a rate of 0.08 inches per year over the past century (Fleenor et al., 2008). In the coming decades, the rate of sea level rise at Golden Gate is projected to further increase. The CALFED independent science board (ISB) has recommended the Delta Vision effort use a mid-range of sea level rise of 8–16 inches by 2050 and 28–39 inches by 2100. A trained ANN (Model 3) was used to test the sensitivity of changes in EC due to sea level rise of 12 inches (1 foot) and 24 inches (2 feet). The results show corresponding increases in EC of approximately 2,500 $\mu\text{S}/\text{cm}$ due to sea level rise of 2 feet and 1,200 $\mu\text{S}/\text{cm}$ due to sea level rise of 1 foot at certain locations (Figure 3-14). The changes are greatest at mid-salinity locations. As noted in the Introduction, data-driven tools such as ANNs are best applied within the envelope of the training data. In this regard, an increase of 1 foot is well within the training range of sea level used, and 2 feet, while on the edge of the training range, may also be acceptable (Figure 3-15). Values of sea level greater than 2 feet are not acceptable for use with these trained ANNs.

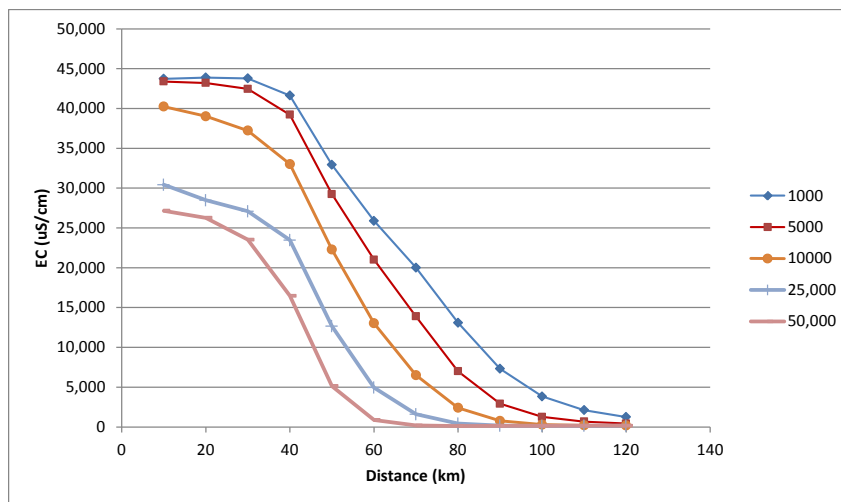


Figure 3-12 Projected EC over distance under different Rio Vista flow conditions (1000, 5000, 10000, 25000, and 50000 cfs).

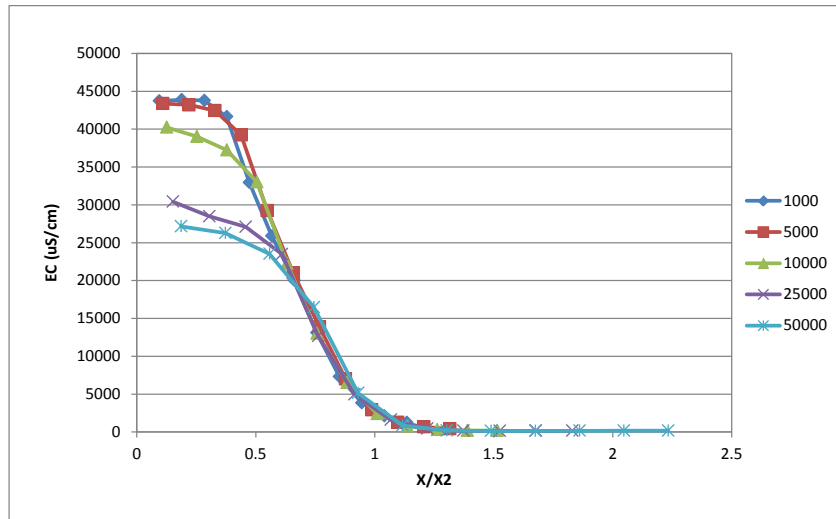


Figure 3-13 Projected EC as a function of standardized distance (X/X2) under different flow conditions.

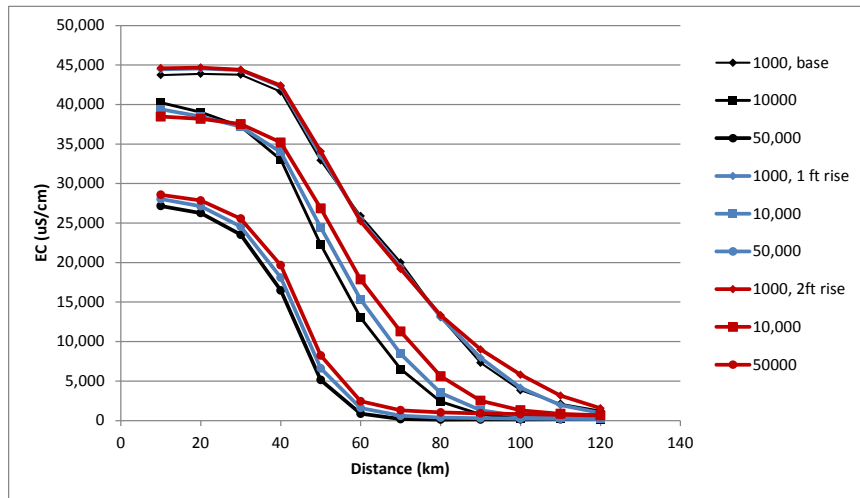


Figure 3-14 Projected EC over distance due to sea level rise of 1 feet and 2 feet under different Rio Vista flow conditions (1000, 10000 and 50000 cfs). Black: base, blue: 1 ft rise, red: 2 ft rise.

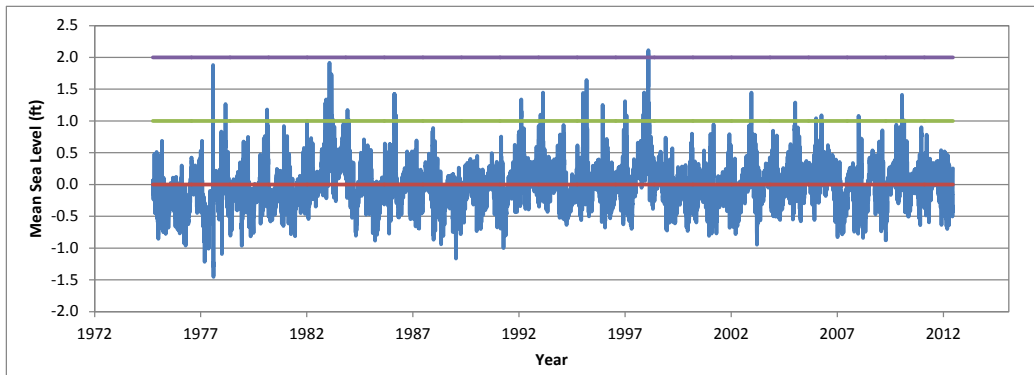


Figure 3-15 Values of sea level used as an input for training. The green and purple lines refer to a change of 1 foot and 2 feet respectively.

3.8 SENSITIVITY TO AIR PRESSURE AND QWEST FLOW

The difference between actual tide and the astronomical tide to a large degree is explained by the air pressure. The air pressure can affect mean sea level. A sensitivity of predicted salinity to air pressure (using Model 3) was performed to evaluate effects of this variable for different values of Rio Vista flow. The sensitivity was performed at a range of air pressure at 1000 mbar, 1015 mbar, and 1030 mbar, bounding the observed air pressure values. The results show a small sensitivity to air pressure, with a slightly greater effect at lower flows, with higher salinity occurring at the same distance for lower pressure (with increased tidal range; Figure 3-16).

A sensitivity analysis was also conducted to evaluate effects of Qwest flow on salinity. Qwest flow reflects diversions from Delta and is a function of Rio Vista flow. A sensitivity of salinity to Qwest flow (using model 3) was performed to evaluate effects of this variable. The sensitivity was performed at a range of Qwest flow at mean levels predicted from the Qwest and Rio Vista flow relationship, and a range of $\pm 14,000$ cfs representing approximately 95% prediction confidence intervals. The results show relatively large sensitivity to Qwest flow under different flow conditions (Figure 3-17).

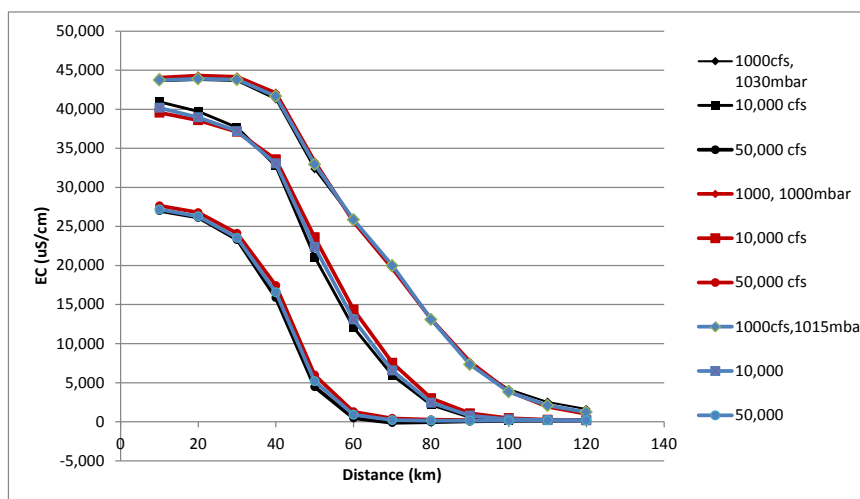


Figure 3-16 Sensitivity of salinity to air pressure (1000, 1015, 1030 mbar), for three different values of Rio Vista flow (1,000, 10,000, and 50,000 cfs).

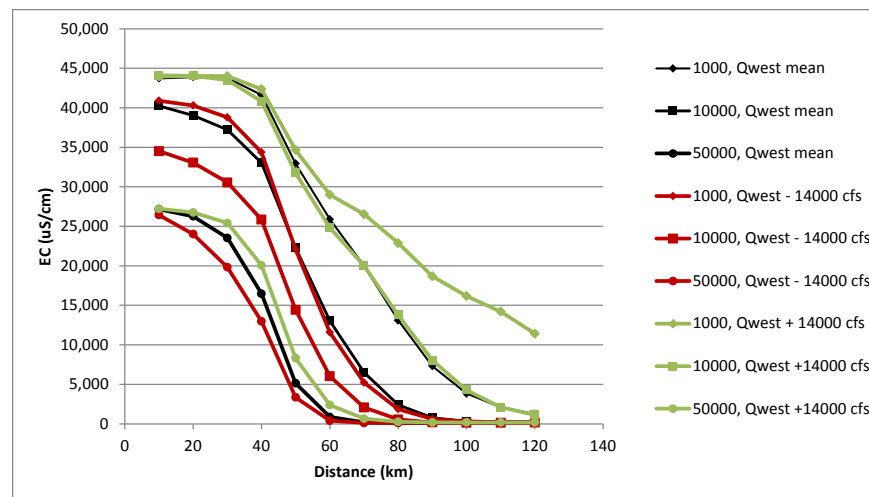


Figure 3-17 Sensitivity of salinity to Qwest flow (mean using relationship between Qwest and Rio Vista flow, mean-14000 cfs, mean + 14000 cfs).

3.9 CHANGES IN X2 DUE TO SEA LEVEL RISE

In this evaluation, the trained ANN model (Model 8 with actual tide at Golden Gate) was used to evaluate possible changes in X2 position due to a median sea level rise of 20 inches. The results show that due to sea level rise, X2 increases, suggesting movement of the X2 position landward (Figure 3-18). The projected changes in X2 range between 0–10 km and can occasionally exceed this range.

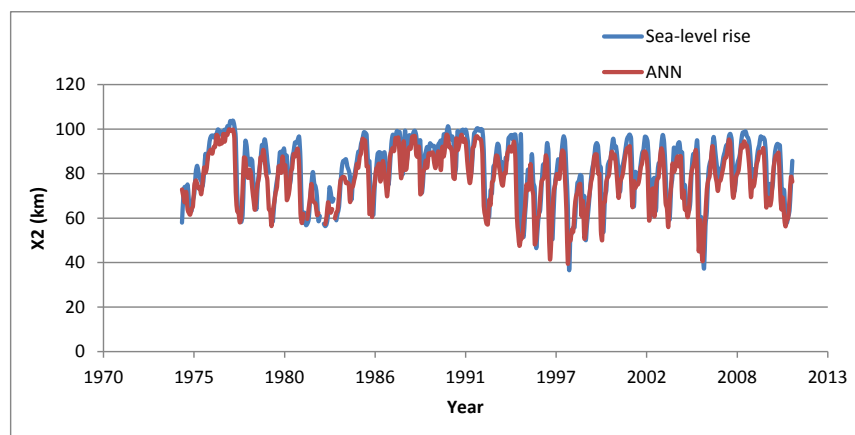


Figure 3-18 Changes in X2 position due to sea level rise of 20 inches.

3.10 APPLICATION TO HISTORICAL SALINITY DATA

A trained ANN (Model 3) was used to generate salinity for the early 20th century period, using flow (Rio Vista and Qwest flow) and tide data from 1929 onwards. This comparison is not a validation of the ANN methodology because operational conditions in the Delta over this period are different from the 1974–2012 training period; however, to the extent that the ANN is an encapsulation of the current conditions in the Delta, the comparison with historical data provides insight into how salinity has changed at certain locations, beyond just changes in the position of specific isohaline positions that has been explored in Roy et al. (2013).

The simulated salinity values from the ANN Model 3 were compared to a reconstructed historical dataset (Roy et al., 2013) in Figure 3-19 to Figure 3-24. Both the ANN models from the Sacramento River (for stations: CLL, EMM and RVB) and the San Joaquin River (for stations: ANH, MRZ, PCT, JER and SAL) were used to hindcast the historical salinity. Generally the ANN model and the reconstructed dataset agreed on the broad temporal patterns in EC at most locations but showed discrepancies in the variations in EC (lower or higher peaks in EC from the historical dataset than the ANN model) at a few locations (e.g., ANH, JER, EMM, and RVB). The agreement between the ANN model and historical dataset at some stations was reasonable with $R^2 = 0.8579$ at MRZ, $R^2 = 0.9018$ at PCT and $R^2 = 0.8172$ at CLL. In several cases, however, there was a marked divergence between ANN predictions and observations for high salinity values, i.e., for the same boundary inputs, the ANN predicted lower salinity than had been observed. In effect, the ANN is confirming the changed spatial pattern in salinities between the training period (1974-2012) and the historical period presented here (1929-1971).

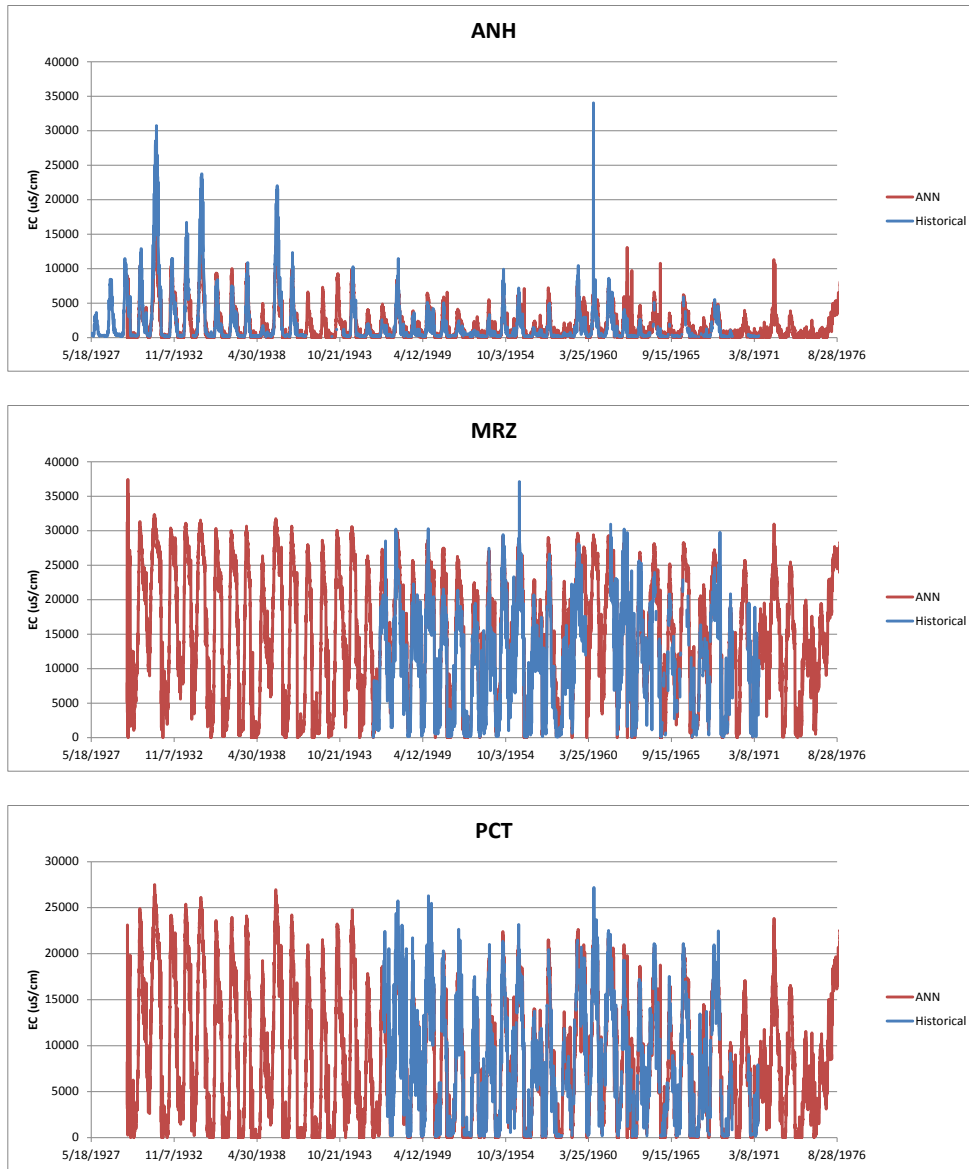


Figure 3-19 Comparison of ANN simulated and reconstructed historical salinity at ANH, MRZ, and PCT.

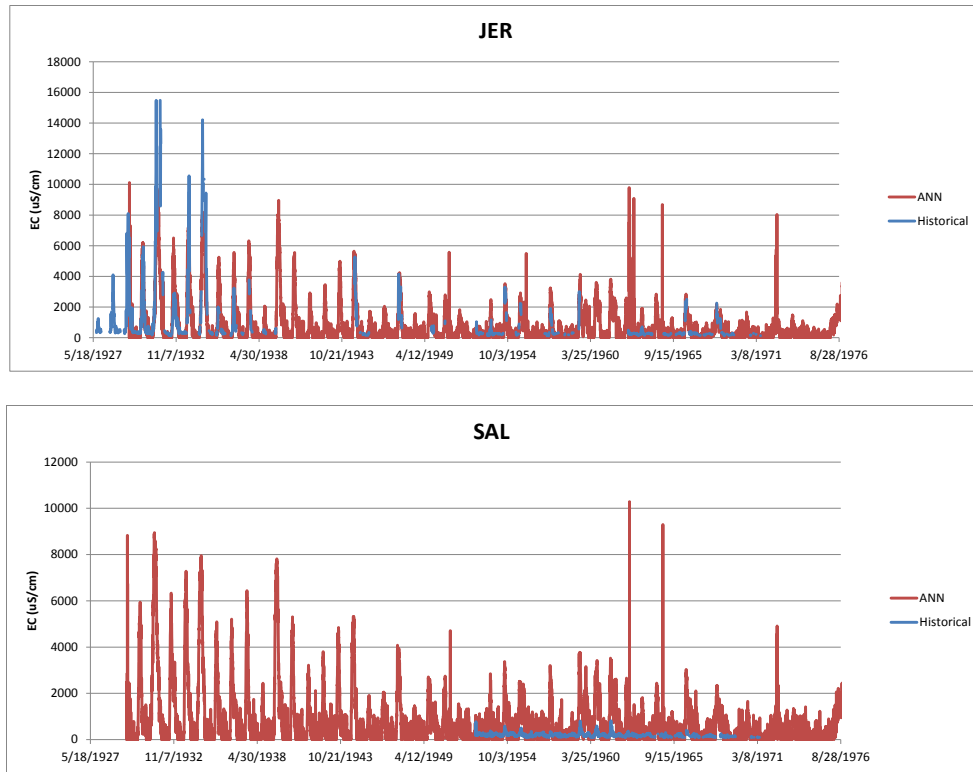


Figure 3-20 Comparison of ANN simulated and reconstructed historical salinity at JER and SAL.

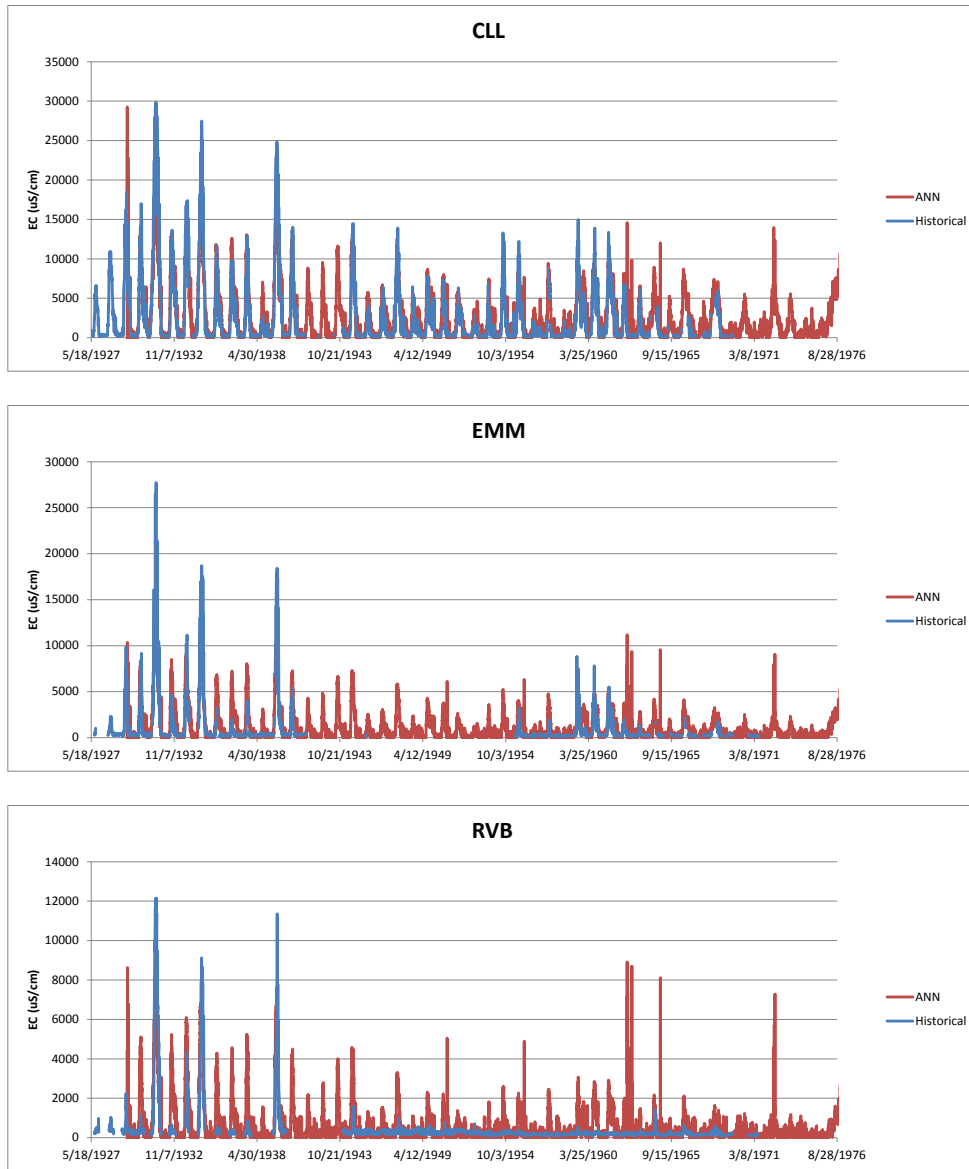


Figure 3-21 Comparison of ANN simulated and reconstructed historical salinity at CLL, EMM and RVB.

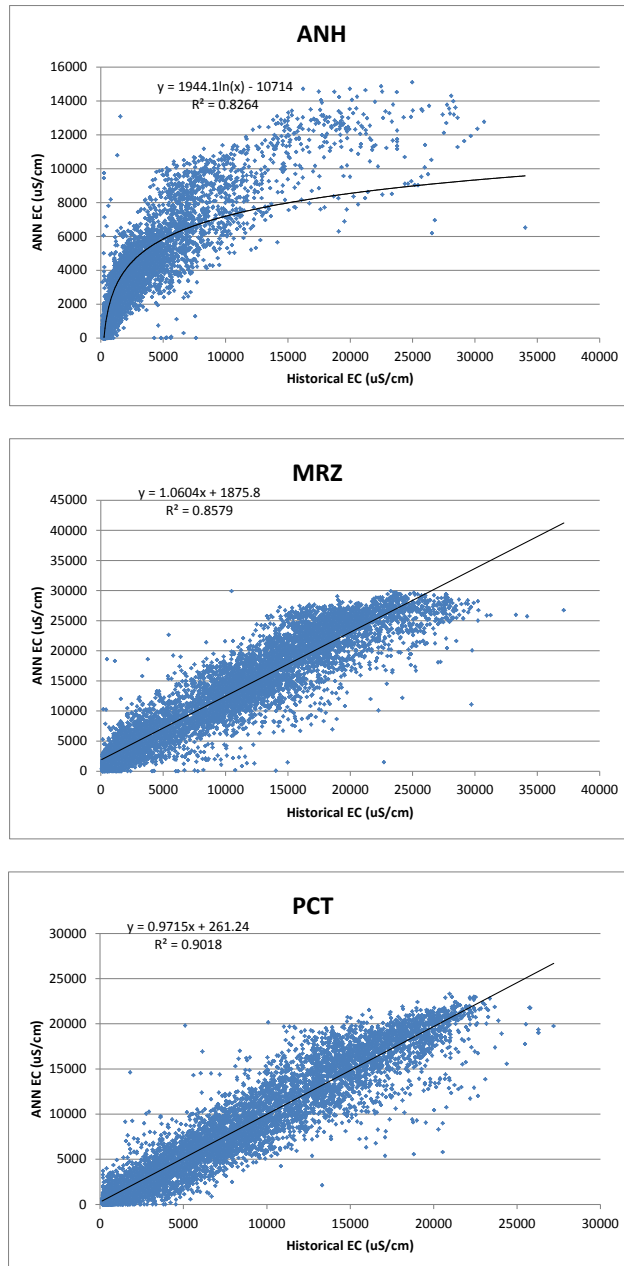


Figure 3-22 Comparison of ANN simulated and reconstructed historical salinity at ANH, MRZ and PCT.

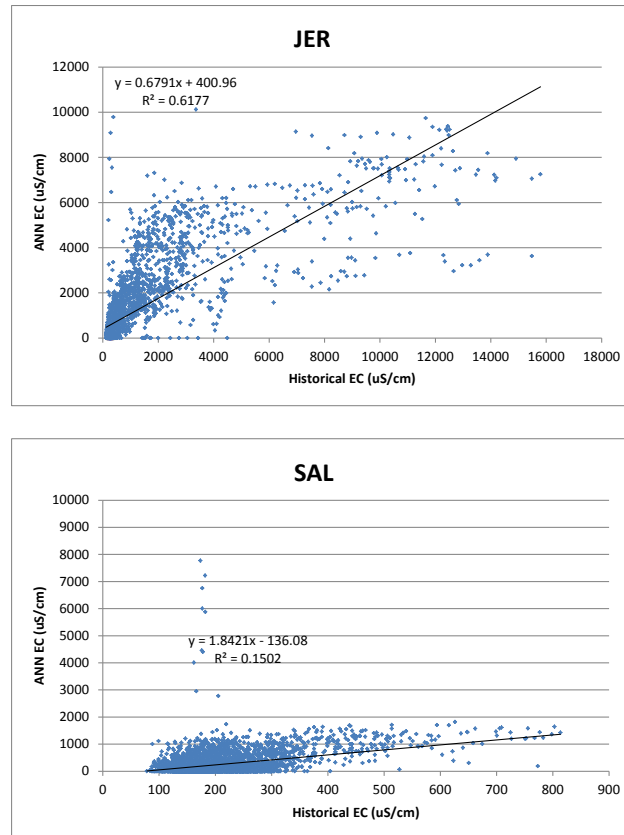


Figure 3-23 Comparison of ANN simulated and reconstructed historical salinity at JER and SAL.

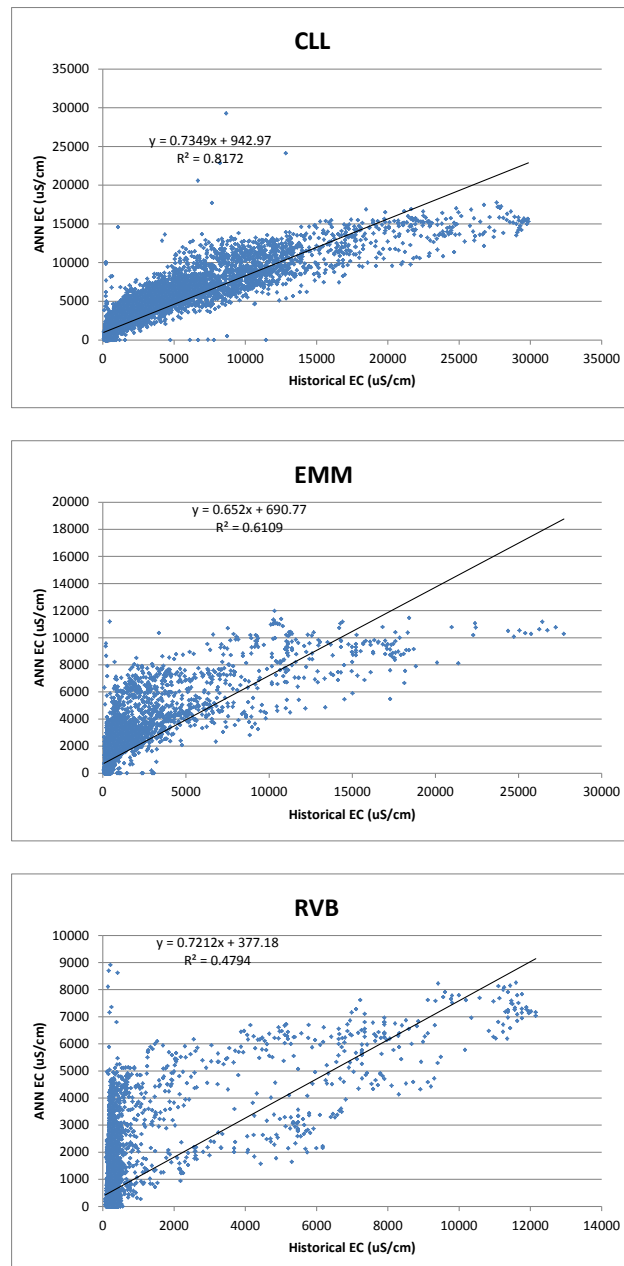


Figure 3-24 Comparison of ANN simulated and reconstructed historical salinity at CLL, EMM and RVB.

3.11 DISTANCE-SALINITY PROJECTIONS USING A TRAINED ANN MODEL

A trained ANN model (Model 3) was applied in a multi-day forecast mode in a manner that would be expected for developing predictions, using data from 2002 as input. In this situation, the model was given appropriate inputs for up to 150 days from a starting point (Jan 2, 2002) the model outputs (with 30 days of prior inputs, from February 1, 2002) were compared to the actual salinity data as a function of distance (Figure 3-25). Good agreement across many days was demonstrated through this exercise giving confidence to its application for future periods.

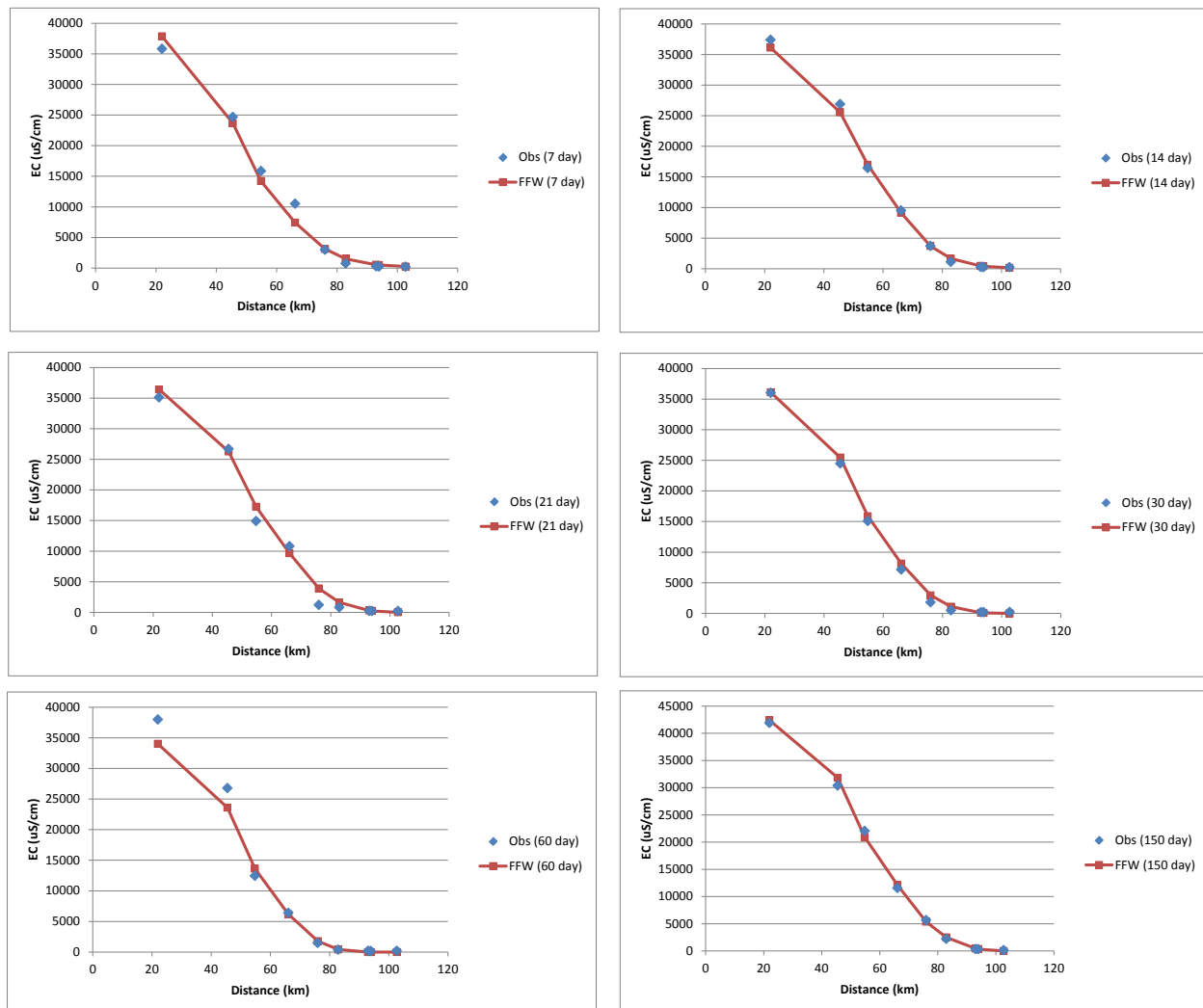


Figure 3-25 Comparison of feedforward ANN (Model 3) forecast and observed salinity from 0 to 150 days.

3.12 LONG TERM SALINITY PROJECTIONS USING FEEDFORWARD AND AUTOREGRESSIVE MODELS

As noted before, for long-term forecasts, an autoregressive model needs to estimate the antecedent salinity, which must be estimated using the model itself. This is somewhat more complex from the input standpoint, and raises the issue of prediction errors that continue to be propagated through time.

An independent evaluation of selected feedforward (Model 3) and autoregressive (Model 9) models was performed by considering their performance over multi-year runs, as might occur during a planning application. Specifically, a 10-year forecast was performed beginning on October 1, 1974. Time series plots for representative stations for both models are shown in Figure 3-26 through Figure 3-29. In general, the autoregressive model does

not perform as well in the forecast mode as was shown in training. In most instances, the feedforward model performs similar or better than the autoregressive model. The main difference between the training and forecast performance of the autoregressive model is the use of observed daily salinity versus model-simulated antecedent salinity, when extended over multiple years.

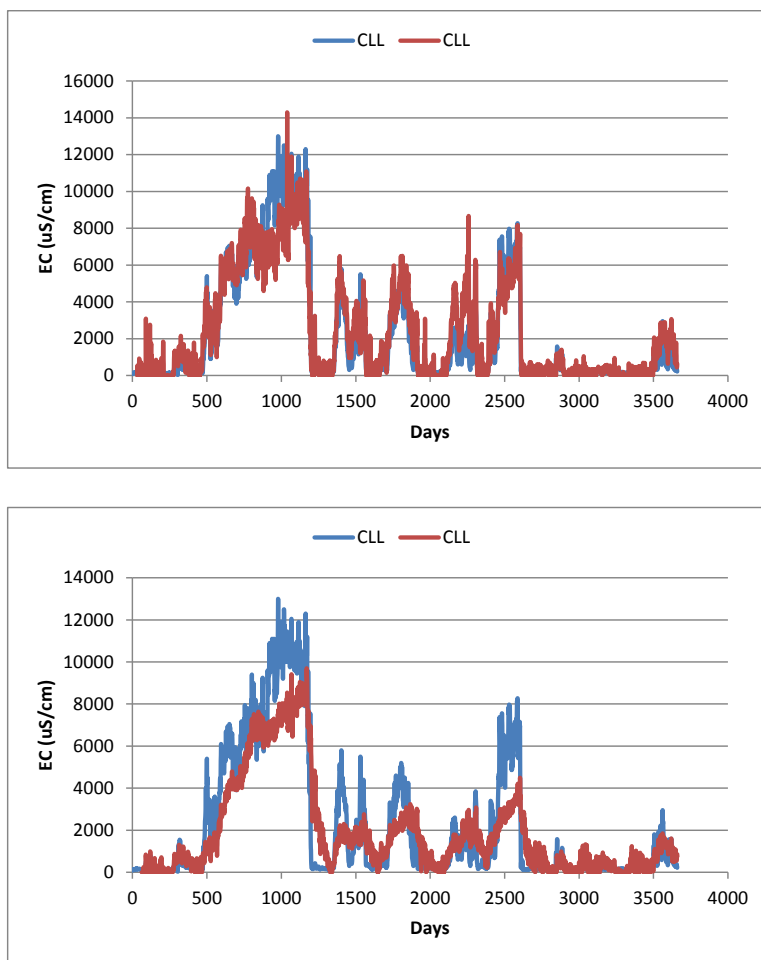


Figure 3-26 Comparison of feedforward ANN (Model 3), upper panel, and autoregressive ANN (Model 9), lower panel, forecast for a 10-year period starting October 1, 1974 (CLL station). Blue = observed data, red = model simulation.

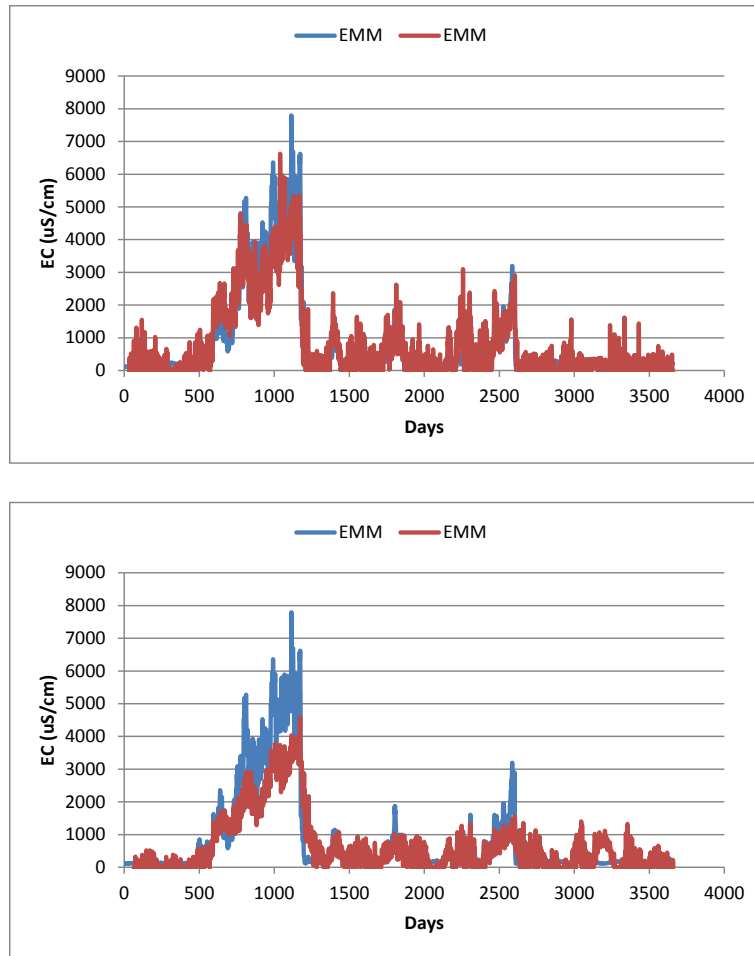


Figure 3-27 Comparison of feedforward ANN (Model 3), upper panel, and autoregressive ANN (Model 9), lower panel, forecast for a 10-year period starting October 1, 1974 (EMM station). Blue = observed data, red = model simulation.

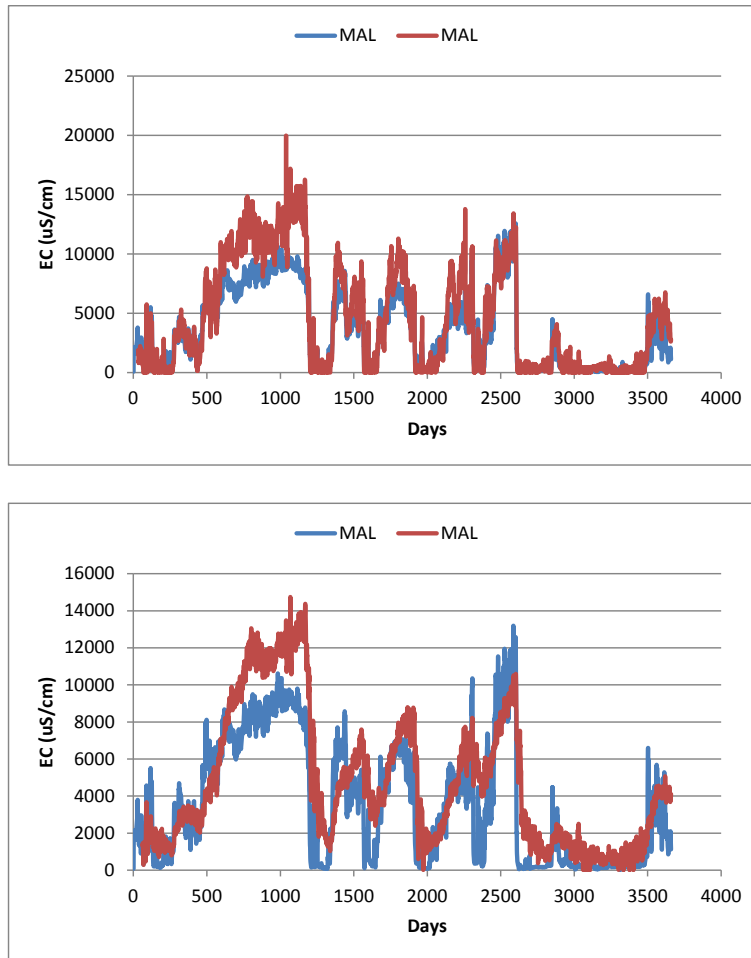


Figure 3-28 Comparison of feedforward ANN (Model 3), upper panel, and autoregressive ANN (Model 9), lower panel, forecast for a 10-year period starting October 1, 1974 (MAL station). Blue = observed data, red = model simulation.

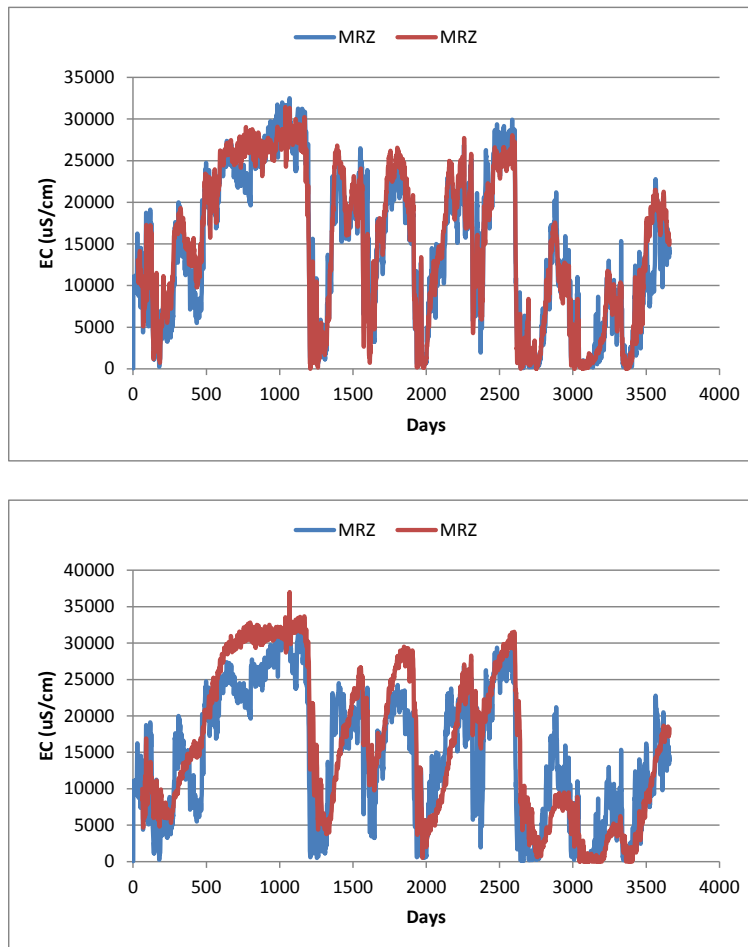


Figure 3-29 Comparison of feedforward ANN (Model 3), upper panel, and autoregressive ANN (Model 9), lower panel, forecast for a 10-year period starting October 1, 1974 (MRZ station). Blue = observed data, red = model simulation.

e

4. SUMMARY AND RECOMMENDATIONS

This work used the four-decade-long record of observed daily salinity in the Western Delta to develop ANNs for salinity as a function of distance using various boundary inputs. Over this period, the system has experienced a range of hydrologic and operational conditions, which are embodied in the trained ANNs. There is confidence that the trained ANNs should represent salinity behavior over a similar range of conditions, although the behavior under conditions that are well outside the training envelope is not well-defined. This limitation applies to all data-driven tools, and the availability of the extensive data set in this region is central to the future utility of the ANN approach. Importantly, this work differs from prior salinity ANN development in the Delta region, where the training has been performed on synthetic data generated from the DSM-2 model (Wilbur and Munevar, 2001; Mierzwa, 2002; Seneviratne et al., 2008).

A major focus of the work was the testing of different input combinations to identify suitable models for predicting salinity as a function of distance. Major inputs that were examined included the following: net Delta outflow, flows past Rio Vista on the Sacramento River and past Jersey Point on the San Joaquin River (identified as Qwest in the DAYFLOW model); tidal terms at different locations and astronomical tide at Golden Gate; and channel depth in the Western Delta. For each combination, two models were developed, one for the Sacramento River and one for the San Joaquin River. The comparison at individual stations as time series and scatter plots was used to evaluate the performance. The outcomes of the training may be summarized as follows:

- An initial evaluation was performed by consideration of the depth term. Over a range of other input combinations, this term was not found to consistently improve model fits. Although a relationship between depth and salinity deviations from the G-model for salinity was noted on an annual basis, it appears that the daily variations in salinity that were the focus of the ANN training may have overwhelmed any gradual changes relating to depth. Based on this initial evaluation the depth term was not considered in subsequent model selection.
- The results suggested that including both Rio Vista and Qwest flows in the training improved the results versus use of only the net Delta outflow term. Models that used both flows as inputs, or those that used the Rio Vista flow and a residual between the Rio Vista-Qwest flow correlation as inputs performed similarly, and either formulation of the flow inputs may be acceptable for future application. For this work, Model 3 (using the Rio Vista-Qwest flow correlation) was highlighted for additional comparison and evaluation.
- The comparison of models with respect to different tidal inputs suggests that relatively good agreement between observed and model predicted values can be achieved through using just one tidal term either as tidal range, the astronomical tide or as the actual tide.

- Including antecedent salinity at Delta stations as an input improved the training results, especially at the eastern locations more distant from the ocean influence.
- Without antecedent salinity as an input, feedforward ANNs with a 30-day delay using the astronomical tide (specifically Model 3) result in relatively good agreement with data across much of the salinity gradient, except lower salinity stations further away from Golden Gate.
- For representative eastern stations, feedforward ANNs were developed specifically for these stations, and shown to perform much better than the distance-salinity ANNs.
- For future application, some combination of distance-salinity and station-specific ANNs may be suitable to best represent the observed values across a wide range of distance from Golden Gate.

The observed data and trained ANNs were compared to three existing models for salinity prediction in the Delta: the K-M model (for X2) and the G-Model (for salinity at fixed locations), both of which were calibrated using data until the early 1990s (Kimmerer and Monismith, 1992; Denton and Sullivan, 1993), and the DSM-2 model for Delta hydrodynamics and water quality. Key aspects of the model inter-comparison may be summarized as follows:

- The K-M model and the G-model performed reasonably well when compared to the overall data set (1974–2012), which typically included two additional decades of data than had been used for the original calibration of the models.
- The trained ANNs displayed better performance compared to the K-M model and the G-Model, when used to predict the relevant quantity (either X2 or salinity). At an eastern station, Jersey Point (JER), the ANN distance-salinity fit was not overwhelmingly better than the G-model. However, in this instance the fits obtained from the station-specific ANNs were considerably better than the G-model results, underscoring the fact that salinity at eastern stations may be affected by key inputs in a different manner than stations closer to the oceanic influence.
- Salinity values at selected eastern stations were fit better using the station-specific ANNs than using DSM2 output at the same locations.
- The X2 position derived from the ANN models for the Sacramento River and the San Joaquin River stations agreed very well with the observed data, and showed better agreement with the observed data than X2 derived from either the K-M model or from the DSM-2 model. The DSM2 model could be used for X2 interpolation only when its position was east of Martinez.

It should be noted that the ANNs provide information that goes beyond existing tools such as the K-M model and the G-model, i.e., information on salinity structure in the estuary (not just X2 position obtained from the K-M model), and information on salinity at arbitrary distances (not calibrated to fixed stations as currently done with the G-Model). The ANN model outputs may be further evaluated against surface salinity results produced from three-

dimensional hydrodynamic models of the Bay (Gross et al., 2007, 2010), although these evaluations were beyond the scope of the present work.

The trained ANNs, specifically one feedforward application and one autoregressive application, were applied in a forecast mode, with predictions made over 10 years given relevant inputs (Models 3 and 9). It was found that over extended periods, the feedforward network made predictions as good as or better than the autoregressive networks, in large part because the autoregressive networks used model-generated antecedent salinity values, and errors in these tend to add to the errors in prediction. Although the long-term application of the autoregressive networks did not exhibit any unstable behavior, the results were not as good as shown during training, when antecedent salinity values were based on actual observations. To address the limitation of the feedforward networks in describing salinity at eastern stations, it is proposed that station-specific salinity ANNs be developed for a limited numbers of stations that are especially important from the standpoint of compliance. While station-specific ANNs are expected to fit data better at all stations (even western stations), they are not suggested as a replacement for the distance-salinity ANNs. This is because, (a) the distance-salinity ANNs are a more efficient representation of the data and encapsulate the behavior across multiple stations, and (b) they can be used to provide insight into the response of the horizontal salinity structure as a function of flow and tidal inputs in a more flexible manner than possible for individual ANNs for each station.

The ANNs trained using the modern EC data were also compared against historical grab sample data that have been compiled in a companion study (Roy et al., 2013). The historical data span 1921 to 1971 and were measured as chlorinity several times each month at different points in the tidal cycle. They were converted to daily average EC using conversion factors for tidal effects and for chloride to EC, and filled using linear interpolation. This hind-cast comparison is not a strict validation of the ANN methodology because operational conditions in the Delta over 1921–1971 are different from the 1974–2012 training period; however, the comparison provides insight into how salinity has changed at certain locations, beyond just changes in the position of the isohalines that has been explored in Roy et al. (2013). The ANN application in this comparison (starting in 1929) showed reasonable fits to values at western (higher salinity) stations, although the performance was poor at eastern (lower salinity) stations. In some cases there was a marked divergence between ANN predictions and observations for high salinity values: for given flows and tides, the ANN model based on current Delta conditions predicted lower salinities than were observed historically.

This study revisited the issue of salinity predictions in the Western Delta using data-driven approaches, as opposed to mechanistic model-based approaches, after a gap of about two decades, during which the quantity of available data has doubled, and tools such as ANNs have become more widespread in the water resources discipline. Using a variety of possible inputs, this work has identified a candidate ANN, noted above as Model 3, that may be applied in a predictive mode in the future for representing the horizontal structure of surface salinity in the estuary. An important finding of this evaluation is that the daily salinity fits are of high enough quality that these may be applied directly for both near-term forecasts as well as aggregated to produce monthly values for long-term planning simulations. Improved

fits at selected eastern stations may be obtained by using station-specific ANNs rather than ANNs that incorporate distance into predictions.

5. REFERENCES

- American Society of Civil Engineers (ASCE). 2000. Artificial Neural Networks in Hydrology, 1. Preliminary Concepts, Vol. 5, No. 2, pp. 115–123.
- Denton, R.A. 1993. Accounting for antecedent conditions in seawater intrusion modeling – applications for the San Francisco Bay-Delta. *Hydraulic Engineering* 93 (1): 448–453. Proceedings of ASCE National Conference on Hydraulic Engineering, San Francisco.
- Denton, R.A. and Sullivan, G.D. 1993. Antecedent flow-salinity relations: application to Delta planning models. Internal CCWD report, 13pp.
- Finch, R. and N. Sandhu. 1995. Artificial neural networks with application to the Sacramento – San Joaquin Delta. California Department of Water Resources Delta Modeling Section, Division of Planning.
- Fleenor, W., E. Hanak, J.R. Lund, J.R. Mount. 2008. Delta hydrodynamics and water salinity with future conditions. Technical Appendix C. in Comparing Futures for the Sacramento–San Joaquin Delta, PPIC report.
- Gross, E. S., Nidzieko, N. J., MacWilliams, M. L., & Stacey, M. T. 2007. Parameterization of Estuarine Mixing Processes in the San Francisco Estuary based on Analysis of Three-Dimensional Hydrodynamic Simulations. In *Estuarine and Coastal Modeling (2007)* (pp. 322–338). ASCE.
- Gross, E. S., MacWilliams, M. L., & Kimmerer, W. J. 2010. Three-dimensional modeling of tidal hydrodynamics in the San Francisco Estuary. *San Francisco Estuary and Watershed Science*, 7(2).
- Harder, J.A. 1977. Predicting estuarine salinity from river inflows, *Journal of the Hydraulics Division, ASCE*, Vol. 103, pp. 877–888.
- Jassby, A.D., W.J. Kimmerer, S.G. Monismith, C.Armor, J.E. Cloern, T.M. Powell, J.R. Schubel and T.J. Vendlinski. 1995. Isohaline position as a habitat indicator for estuarine populations. *Ecological Applications* 5: 272–289.
- Kimmerer, W. and S. Monismith. 1992. An estimate of the historical position of 2ppt salinity in the San Francisco Bay Estuary. Issue Paper prepared for the fourth technical workshop on salinity, flows and living resources of the San Francisco Bay/Delta estuary. August 1992.
- List, John. 1994. X2 and the X2/Net Delta Outflow Relationship. Prepared for California Urban Water Agencies, Sacramento, California.

- Maier, H.R., A. Jain, G.C. Dandy, K.P. Sudheer. 2010. Methods used for the development of neural networks for the prediction of water resource variables in river systems: current status and future directions. *Environmental Modeling and Software* 25: 891–909.
- Mierzwa, M. 2002. Chapter 4: CALSIM versus DSM2 ANN and G-model Comparisons. Methodology for flow and salinity estimates in the Sacramento–San Joaquin Delta and Suisun Marsh. 23rd Annual Progress Report. June 2002.
- Monismith, S. G., Kimmerer, W., Burau, J. R., & Stacey, M. T. 2002. Structure and flow-induced variability of the subtidal salinity field in northern San Francisco Bay. *Journal of Physical Oceanography*, 32(11), 3003-3019.
- Roy, S.B., J. Rath, L. Chen, M.J. Unga. 2013. Salinity trends in the Western Delta (1921–2012). Draft report to San Luis and Delta Mendota Water Authority and Metropolitan Water District of Southern California.
- Schemel, L. 2001. Simplified conversion between specific conductance and salinity units for use with data from monitoring stations. *IEP Newsletter* Volume 14, Number 1, Winter 2001.
- Senevirante, S., S.Wu, and Y. Liang. 2008. Chapter 3: Impacts of Sea Level Rise and Amplitude Change on Delta Operations. Methodology for flow and salinity estimates in the Sacramento – San Joaquin Delta and Suisun Marsh. 29th Annual Progress Report. June 2008.
- Wilbur, R. and A. Munevar. 2001. Chapter 7: Integration of CALSIM and Artificial Neural Networks Models for Sacramento–San Joaquin Delta Flow-Salinity Relationships. Methodology for flow and salinity estimates in the Sacramento–San Joaquin Delta and Suisun Marsh. 29th Annual Progress Report. June 2008.